

Impact of Gradation and Moisture Content on Stiffness Parameters of Base Materials

Final Report
January 2016

Prajwol Tamrakar
Graduate Research Assistant

Soheil Nazarian
Professor, Department of Civil Engineering

University of Texas at El Paso
500 W University Ave, El Paso, TX 79968

External Project Manager
Richard Izzo
Texas Department of Transportation

In cooperation with
Rutgers, The State University of New Jersey
And
State of Texas
Department of Transportation
And
U.S. Department of Transportation
Federal Highway Administration

Disclaimer Statement

The contents of this report reflect the views of the authors, who are responsible for the facts and the accuracy of the information presented herein. This document is disseminated under the sponsorship of the Department of Transportation, University Transportation Centers Program, in the interest of information exchange. The U.S. Government assumes no liability for the contents or use thereof.

TECHNICAL REPORT STANDARD TITLE PAGE

1. Report No. CAIT-UTC-054	2. Government Accession No.	3. Recipient's Catalog No.	
4. Title and Subtitle Impact of Gradation and Moisture Content on Stiffness Parameters of Base Materials		5. Report Date January 2016	
		6. Performing Organization Code CAIT/UTEP	
7. Author(s) Prawjol Pamrakar, Soheil Nazarian		8. Performing Organization Report No. CAIT-UTC-054	
9. Performing Organization, Name and Address University of Texas at El Paso 500 W University Ave, El Paso, TX 79968		10. Work Unit No.	
		11. Contract or Grant No. DTRT12-G-UTC16	
12. Sponsoring Agency Name and Address Center for Advanced Infrastructure and Transportation Rutgers, The State University of New Jersey 100 Brett Road Piscataway, NJ 08854		13. Type of Report and Period Covered Final Report 1/1/15 - 12/31/2015	
		14. Sponsoring Agency Code	
15. Supplementary Notes U.S Department of Transportation/Research and Innovative Technology Administration 1200 New Jersey Avenue, SE Washington, DC 20590-0001			
16. Abstract The performance of flexible pavement depends on the mechanical characteristics of its base layer. The mechanical characteristics such as stiffness and deformation resistance depend on many factors such as the material gradation fines content, moisture content, physical properties of coarse aggregate and more. The gradation of material could change due to improper material handling, migration of fines from subgrade and the other reasons. Similarly, the moisture content of base materials may alter during pavement construction and operation by exposure to excessive water and percolation of rainwater from pavement surface. In this research, the roles of gradation, fines content and moisture content were evaluated to understand the effects on the mechanical characteristics of base. Twelve different tests sequences were performed with a combination of moisture contents from dry to wet of optimum moisture content and fine contents. The increase in moisture content typically had detrimental effect on the mechanical characteristics of the base material. However, the increase in fines (change in gradation) showed mixed results on the mechanical characteristics.			
17. Key Words Flexible pavement, Unbound granular base, Fines content, Material gradation, Performance of pavement		18. Distributional Statement	
19. Security Classification Unclassified	20. Security Classification (of this page) Unclassified	21. No. of Pages 57	22. Price

Acknowledgments

The authors would like to thank Rutgers Center for Advanced Infrastructure and Transportation (CAIT) for supporting this project. The successful progress and completion of this project could not have happened without the help and input of many staffs and students of Center for Transportation Infrastructure Systems (CTIS). The authors also like to acknowledge Executive Director of CTIS, Imad Abdallah, Laboratory Manager, Jose Garibay and undergraduate students, Yair Morales, Jose Luis, Jannet Hernandez, Miguel Antonio Perez and Uriel Rocha.

Table of Contents

Table of Contents	v
List of Figures	vi
List of Tables	viii
Chapter 1 – Introduction	1
Statement of Problem.....	1
Objective and Scope	3
Organization of Report	4
Chapter 2 – Background	5
Factors Affecting Stiffness of Base Materials	5
Roles of Fines Content, Gradation and Moisture Contents of Base Materials	5
Base Material Characterization for Design and Construction	7
Methodology for Characterizing Base Materials.....	8
Traditional Tests for Unbound Granular Materials	9
Nondestructive Tests for Unbound Granular Materials.....	11
Performance Tests for Unbound Granular Materials.....	13
Previous Studies at UTEP.....	15
Chapter 3 – Research Approach and Testing Procedure	17
Materials for Tests	17
Test Procedure	19
Moisture-Density and Moisture-Modulus Relationships.....	19
Laboratory Mechanical Properties Tests	20
Small-Scale Test	20
Chapter 4 – Results from Laboratory and Small-Scale Tests.....	24
Laboratory Tests	24
Unconfined Compression Tests	24
FFRC Tests	25
Permanent Deformation Tests.....	25
Resilient Modulus Tests.....	27
Small-Scale Tests.....	27
PSPA Tests.....	27
LWD Tests	28
Cyclic Modulus Tests	29
Cyclic Stage Tests.....	31
Comparison of Laboratory and Small-Scale Tests	33
Effect of Moisture Content on Laboratory Tests	33
Effect of Moisture Content on Small-Scale Tests.....	34
Correlation of Laboratory Tests.....	35
Correlation of Small-Scale Tests	35
Correlation of Laboratory Test and Small-Scale Tests.....	36
Chapter 5 – Summary and Conclusions.....	43
References.....	44

List of Figures

Figure 2.1 Unconfined compression test: a) Test setup and b) Typical output	10
Figure 2.2 Resilient Modulus and Permanent Deformation Test: a) Test setup, b) Specimen response during Resilient Modulus Test (From Buchanan 2007) and c) Typical result obtained from Resilient Modulus Test	11
Figure 2.3 The FFRC test (left) and output of the test (right).....	12
Figure 2.4 Portable Seismic Property Analyzer.....	13
Figure 2.5 Light Weight Deflectometer.....	14
Figure 2.6 Principle of Plate Load Test Apparatus (from Sweere 1990).....	14
Figure 3.1. Particle size distribution for material mixes of different fines contents.....	18
Figure 3.2 Moisture-density relationships for bases various fines contents	19
Figure 3.3 Typical moisture-density and moisture-modulus relationships.....	19
Figure 3.4 Schematic for tank cross-section for a small-scale test	20
Figure 3.5 Small-scale test with a MTS system- a) Plate load test, and b) Three different plates for plate load tests.....	21
Figure 3.6 Typical load-deformation responses from the cyclic-modulus test: a) applied loads and b) measured deformations.....	22
Figure 3.7 Typical load-deformation responses from the cyclic-stage test for a) cyclic ramp load and b) continuous load.....	22
Figure 3.8 Small-scale test with LWD.....	23
Figure 3.9 Small-scale test with PSPA	23
Figure 4.1. Unconfined compressive strength (USC) of standard specimens: a) grouped by fines content and b) grouped by moisture content.....	24
Figure 4.2 FFRC modulus of standard specimens: a) grouped by fines content and b) grouped by moisture content.....	25
Figure 4.3. Strains measured at different loading cycles on standard specimens in permanent deformation tests	26
Figure 4.4 Resilient strains of standard specimens: a) grouped by fines content and b) grouped by moisture content. Permanent strains: c) grouped by fines content and d) grouped by moisture content.....	26
Figure 4.5 Representative resilient modulus (MR) of standard specimens: a) grouped by fines content and b) grouped by moisture content.....	27
Figure 4.6 PSPA modulus of large specimens: a) grouped by fines content and b) grouped by moisture content.....	28
Figure 4.7 PSPA modulus of subgrade	29
Figure 4.8 LWD modulus of large specimens: a) grouped by fines content and b) grouped by moisture content.....	29
Figure 4.9 LWD modulus of subgrade	30
Figure 4.10 Cyclic modulus of large specimens from cyclic modulus test using 4” diameter plate: a) grouped by fines content and b) grouped by moisture content.....	30
Figure 4.11 Cyclic modulus of large specimens from cyclic modulus test using 8” diameter plate: a) grouped by fines content and b) grouped by moisture content.....	31
Figure 4.12. Cyclic modulus of large specimens from cyclic modulus test using 12” diameter plate: a) grouped by fines content and b) grouped by moisture content.....	32
Figure 4.13 Load-deformation response of large specimens from cyclic stage test.....	33

Figure 4.14 Stiffness of large specimens from cyclic stage test: a) grouped by fines content and b) grouped by moisture content.....	34
Figure 4.15 Permanent deformation of large specimens from cyclic stage tests: a) grouped by fines content and b) grouped by moisture content.....	35
Figure 4.16. Variations in normalized moduli, UCS and permanent deformation with normalized moisture content in laboratory tests: a) FFRC Test, b) Unconfined Compression Test, c) Resilient Modulus Test and d) Permanent Deformation Test.....	36
Figure 4.17 Variations in normalized modulus, permanent strain and stiffness with measured moisture content in small-scale tests: a) LWD Test, b) PSPA Test, c) Cyclic Modulus Test (CST) showing stiffness and d) CST showing permanent strain.....	37
Figure 4.18 Variation in moduli and UCS of specimens in laboratory tests: a) Resilient Modulus (MR) Test and FFRC Test, b) MR Test and Unconfined Compression Test (UCT), and c) UCT and FFRC Test.....	38
Figure 4.19 Variations in modulus of large specimens in small-scale tests with different loading plates at different peak contact pressures: a) 30 psi, b) 50 psi, c) 70 psi and d) 90 psi	39
Figure 4.20 Variations in the LWD modulus and stiffness of large specimens measured through cyclic stage test in small-scale tests.....	40
Figure 4.21 Variations in permanent strains of laboratory tests and small-scale tests:	40
Figure 4.22 Variation of k-parameters with permanent strain measured from laboratory test (a, b and c). Variation of k-parameters with permanent strain measured in small-scale test (e, f and g).....	41
Figure 4.23 Variations in the PSPA modulus from small-scale test with the FFRC modulus from the laboratory test.....	42

List of Tables

Table 1.1 Summary of Flexible Pavement Distress, Contributing Factors and Related Test Parameters (Saeed et al. 2001).....	2
Table 2.1. Tests for Unbound Granular Materials (from Saeed et al. 2001)	9
Table 2.2 Loading sequences for Resilient Modulus (MR) and Permanent Deformation (PD) Tests (From Gandara 2004).....	12
Table 3.1 Overall tests of base materials at different fines contents and moisture contents	17
Table 3.2. Particle size distribution of mixes.....	18
Table 3.3 Soil classifications for base materials.....	18

Chapter 1 – Introduction

Stresses and deformations in the layers of a pavement due to vehicle loads decrease gradually with depth. The capability of the base layer to distribute safely the stresses from the surface course to the subgrade affects the satisfactory performance and life span of the pavement. The amount of fines (aggregates passing sieve number 200 or smaller than 75 micron) and water content of the base play important roles in achieving satisfactory performance. Fines, especially plastic fines, have a detrimental effect on the mechanical properties of the base layers. Although the moisture content is controlled during construction, the moisture level can vary during the pavement operation phase due to the climatic changes. During the rainy season, the pavement layers are subjected to high moisture contents. After evaporation and drainage, the moisture content may drastically reduce below the optimum level. These variations in moisture content are likely to affect the material properties and pavement performance. Intrusion of excessive moisture in the geomaterials with plastic fines results in a softening behavior that affects the material properties negatively. It is essential to understand the effects of fines and moisture content on the strength characteristics of base materials.

The mechanical characteristics of the geomaterials such as Young's modulus and shear strength depend on many factors such as the material gradation, fines content, moisture content, physical properties of coarse aggregates (e.g., surface roughness and hardness), type of aggregates (e.g., crushed or uncrushed), mineralogy of aggregates, plasticity of fines and more. The base is a critical layer to maintain the stability of the pavement. In this research, the mechanical characteristics of the base materials are investigated through laboratory and small-scale tests. Laboratory tests include the index and mechanical tests that ensure the quality of the available material for pavement construction. Small-scale tests include the scenarios that resemble tests under controlled field conditions for quality control purposes.

Statement of Problem

Historical data pertaining to the evaluation of pavement performance have shown that most pavement distresses originate from the underlying pavement layers. Table 1.1 provides a summary of these distresses that was originally reported by Saeed et al. (2001). For example, one of the common distresses in flexible pavements is rutting. Rutting refers to a surface depression in the wheel path on the pavement surface that is caused by the accumulation of permanent deformations of the pavement layers (Simpson 1999). Permanent deformation of base occurs due to insufficient compaction, excessive moisture content and/or poor material quality (Fleming et al. 2000). Fine aggregate particles (fines) in an unbound aggregate base contribute to attaining sufficient compaction level, and hence, provide stability to the pavement system. Excessive fines in the base increase the moisture susceptibility and result in the reduction of stiffness properties. The presence of excessive fines in unbound aggregate base can be due to segregation of material during pavement construction or contamination of material from underlying subgrade soil during pavement life.

Table 1.1 Summary of Flexible Pavement Distress, Contributing Factors and Related Test Parameters (Saeed et al. 2001)

Type of Distress	Description of Distress	Base Failure Manifestation	Contributing Factors	Possible Related Test Parameter
Fatigue Cracking (Alligator Cracking)	Appears as fine, longitudinal hairline cracks parallel to one another in the wheel path in the direction of traffic. Progression of distress is signaled by interconnection of cracks forming many-sided, sharp angled pieces. As cracks become wider, spalling may occur.	High deflection/strain in the asphalt concrete surface due to lack of base stiffness. Alligator cracking only occurs in areas where repeated wheel loads are applied. High flexibility in the base or inadequate thickness of base allows for excessive bending strains in the asphalt concrete surface. Changes in base properties with time can render the base inadequate to support loads.	Low modulus Improper gradation High fines content High moisture level Lack of adequate particle angularity and surface texture. Degradation under repeated loads and freeze-thaw cycling.	Resilient Modulus Gradation & fines content Frost susceptibility Density
Rutting/ Corrugations	Long surface depressions in the wheel path that may not be noticeable except during and following rains. Pavement uplift may occur along the sides of the rut. Resulting from permanent deformation in one or more pavement layers or subgrade, usually caused by consolidation and/or lateral movement of the materials due to load.	Lateral displacement of particles with applications of wheel loads due to inadequate shear strength resulting in a decrease in the base layer thickness. Consolidation of the base due to inadequate initial density or changes in base properties with time due to poor durability or frost effects may also cause rutting.	Low shear strength Low density of base material Improper gradation High fines content High moisture level Lack of adequate particle angularity and surface texture. Degradation under repeated loads and freeze-thaw cycling.	Triaxial Testing – angle of internal friction, cohesion Gradation Fines content
Depressions	Depressions are localized low areas in the pavement surface caused by settlement of the foundation soil or consolidation in the subgrade or base/ subbase layers due to improper compaction.	Inadequate initial compaction or nonuniform material conditions results in additional reduction in volume with load applications. Changes in material conditions due to poor durability or frost effects may also result in localized densification with eventual fatigue failure.	Low density of base material	Density
Frost Heave	Frost heave appears as an upward bulge in the pavement surface and may be accompanied by surface cracking resulting in potholes. Freezing of underlying layers resulting in an increased volume of material causes the upheaval. An advanced stage of distortion mode of distress resulting from differential heave is surface cracking with random orientation and spacing.	Ice lenses are created within the base/subbase during freezing temperatures, particularly when freezing occurs slowly, as moisture is pulled from below by capillary action. During spring thaw large quantities of water are released from the frozen zone, which can include all unbound materials.	Freezing temperatures Source of water Permeability of material high enough to allow free moisture movement to the freezing zone.	Gradation Fines Content Fines Type

The combined effects of excessive fines and moisture content can be detrimental in cold climates. Konrad and Lemieux (2005) studied the influence of fines on the frost susceptibility of geomaterials in the laboratory using freezing tests. The authors considered granitic (non-plastic) fines and kaolinite clay (plastic) fines. They found that the frost susceptibility of the aggregates increases with both types of fines.

A survey of the State Departments of Transportation (DOTs) of the United States and transportation agencies of Canada by Tutumluer (2013) found that 33 out of 46 respondents limit the amount of fines in the base to less than 12% while five respondents allow more than 15% fines. Some of respondents indicated that they did not differentiate between plastic and non-plastic fines. The degree of variation in the stiffness properties of the base materials should be assessed to determine the optimal amount of fines. The main purpose of this research is to understand the role of fines with combination of various moisture contents in the mechanical properties of the base layers.

Objective and Scope

Performance of pavements is affected mainly by the properties of the pavement layers, the vehicle loading characteristics and the climatic conditions. The properties of the pavement layers include the strength characteristics such as deformation resistance and shear strength. The vehicle loading characteristics include axle weight, tire pressure, contact area, rate of loading and vehicle speed. The climatic conditions include temperature, precipitation, humidity, ultra-violet index, wind speed and ground water table.

Although the performance of pavements is influenced by multiple factors, this research is focused on understanding the role of the base layer to maintain the stability of pavement systems. The main factors influencing the responses of the base layer during construction and operation phases are vehicle loading characteristics, precipitation and ground water table, and the strength characteristics. The vehicle loading characteristics affect the magnitude of the stresses experienced by the base whereas the climatic conditions affect the variation in its moisture content and stiffness. Due to combined effects of vehicle loadings and climatic conditions, it is desirable to evaluate the stiffness parameters (e.g., modulus, and permanent deformation resistance) of the base materials, and to model their effects on the pavement performance and the estimated life of pavements.

Laboratory tests were performed to observe the responses of base layers due to variations in the fines content and moisture content. Small-scale tests were performed under the same material conditions as the laboratory tests to measure the responses of the base layers. The objectives of this research can then be categorized in the following bullets:

- To evaluate the stiffness parameters of base materials with various fines contents and moisture contents;
- To understand the impact of the variations in fines content and moisture content of base materials on their performance;
- To develop a relationship among the stiffness parameters, fines content and moisture content; and
- To correlate the stiffness parameters obtained from the laboratory and field methods.

Organization of Report

This report consists of four chapters besides this introductory chapter. Chapter 2 provides background information and review of the literature related to the characteristics of unbound granular materials used as road base and methods for characterizing those materials.

Chapter 3 describes the research approach and testing procedures for the project. It explains the procedure of preparing different aggregate mixes for testing. The mixes are differentiated by the percentage of fines content. This chapter also explains the ranges for varying the moisture contents of the mixes. The types and procedures of different tests for the laboratory and the small-scale tests are also explained in that chapter.

Chapter 4 presents the results from the laboratory and small-scale tests. In addition, comparisons of the laboratory and the small-scale tests are provided to understand how the outcomes of the laboratory tests reflect on the field performance.

Chapter 5 contains a summary of findings and conclusions drawn from this research project.

Chapter 2 – Background

This chapter focuses on the review of the literature with an emphasis on the behavior of the base materials, the role of fines content and moisture content on mechanical characteristic of bases, various challenges associated with base materials during design and constructions, and the methods for characterizing base materials.

Factors Affecting Stiffness of Base Materials

The load distribution mechanism in mechanically stabilized bases depends on particle interlocking and particle friction. The stresses experienced by the base layer mainly due to the moving vehicles are not uniform; rather the stresses are concentrated along load carrying particle chains formed by the coarse aggregates. Mechanical behavior of unbound granular bases is influenced by parameters such as stress sensitivity, nonlinearity, and anisotropy (Karasahin et al. 1993).

Stress sensitivity is associated with hardening and softening behaviors of material under repeated vehicle loads (Von Quintus and Killingsworth 1998). The hardening behavior results in a greater strength and stiffness under the repeated loads. Similarly, the softening behavior results in the reduction in the material strength or stiffness. The repeated load triaxial test (e.g., resilient modulus test) can be used to characterize the hardening and softening behaviors of base materials.

Nonlinearity refers to the response of the material in terms of strain due to an applied stress. A base layer has a linear response for small strains and nonlinear response at higher strains. Ishihara (1996) mentioned that soils exhibit linear elastic behavior below a strain of $10^{-2}\%$ and nonlinear elasto-plastic behavior in the strain range of $10^{-2}\%$ to 1%. The magnitude of the strain experienced by a base layer is a function of the applied load and mechanical characteristics of the pavement layers. Sawangsuriya et al. (2006) stated that a typical range of strains experienced by bases is $10^{-2}\%$ to 1% that falls under a nonlinear response range.

Anisotropy is about the differences in the behavior of a material in different directions. The anisotropy can be either inherent or load induced (Salehi et al. 2008). The inherent anisotropy is due to the orientation of coarse aggregates in the base layer; whereas the load-induced anisotropy is related to the magnitude of stress or strain in various orientations at a location within the base layer due to moving vehicle load.

Gradation, moisture content and degree of compaction of base materials affect their constitutive models, and hence, their stiffness. Richter (2006) and Cary and Zapata (2010) discussed the impact of moisture content on the in-situ moduli of the pavement materials. The other factors that can also affect the stiffness of the base materials are surface roughness, angularity and asperity of the aggregates. Pan et al. (2006) studied the aggregate morphological indices of pavement geomaterials with an image analysis approach. They observed that the resilient modulus noticeably increased when the aggregate angularity and surface roughness increased.

Roles of Fines Content, Gradation and Moisture Contents of Base Materials

Thompson and Smith (1990) and Tian et al. (1998) showed that fines content can affect the strength of road construction materials. The alternation of fines content in a base material may result in

different packing order and void distribution and packing density. Other factors, such as the maximum aggregate size, particle size distribution of coarse aggregate and shape of coarse aggregate, also play important roles in the achieved packing density. One of the methods of estimating the packing density is by measuring the “fine fraction porosity” that is a ratio between the total voids in the aggregate matrix and the total voids if the entire matrix comprised of the coarse particles only (Bilodeau et al. 2009). The change in the material gradation due to the variation in the fines content has the potential to replace the contact spaces between the aggregates by the fines. This phenomenon may alter the load carrying capacity through particle-to-particle contacts in an aggregate matrix. The permeability of a material decreases, and its frost susceptibility and moisture susceptibility increase with an increase in the material packing density. As such, base materials with high fines contents are not suitable for drainage and frost-protection purposes.

Hicks and Monismith (1971) reported that the resilient modulus of partially crushed aggregates with fines contents in excess of 10% was lower than the fully crushed aggregates with the same amount of fines. They indicated that crushed aggregates with more surface contact points contributed to the increased resilient modulus behavior. However, that effect on the resilient modulus was minimal when the fines content was in the range of 2% to 10%. Jorenby and Hicks (1986), Kamal et al. (1993) and Lekarp et al. (2000) reported that the voids in the aggregate mix prepared from well-graded aggregates were usually replaced by fines to a certain level, and this phenomenon attributed to an increase in the resilient modulus. On the contrary, Barskale and Itani (1989) observed a significant reduction in the resilient modulus when the fines content increased from 0% to 10%.

Yideti et al. (2014) studied the role of particle size and shape of granular materials and their impacts on the resilient behavior of the base materials. The authors adopted a packing theory approach to understand the influence of the porosity of the material posed by the granular materials on the deformational behavior of the entire pavement structure. The following three key parameters were used for studying the resilient behavior:

- Primary structure (coarse grain particles that form the load-carrying network of unbound granular materials),
- Primary structure porosity (the fraction of the volume of voids in the primary structure over the total volume of granular mix) and
- Coordination number (the average number of contact points per particle of primary structure as a function of porosity).

The authors observed an increase in the resilient modulus of the materials with primary structure porosities between 32% and 47% (coordination number between 9.6 and 6.4) and a decrease in the resilient modulus for primary structure porosities greater than 50% (coordination number less than 6). They concluded that the fines that fill the pore spaces and decrease the primary structure porosity could contribute to the increment of resilient modulus of the base materials.

The variation in the material gradation impacts the pavement design and construction procedures (Thom and Brown 1988; Dawson et al. 1996; and Lekarp 1999). The studies performed by Kolisoja (1997) using aggregates with similar grain size distributions and fines contents showed that the resilient modulus increased with increasing the maximum particle size. An increase in the particle

size decreased the particle-to-particle contact resulting in a lower total deformation and consequently a higher stiffness.

Santha (1994); Malla and Joshi (2008); and Yau and Quintus (2002) worked extensively to estimate the resilient modulus of granular materials based on their gradations. Those studies demonstrated that the resilient behaviors of the base materials measured with the repeated axial stress or resilient modulus testing methods were influenced by the fines content. Gidel et al. (2001) stated that the permanent deformation of pavement layers could be controlled by adopting a well-graded gradation of the unbound granular materials and introducing about 6% to 10% fines to achieve a high density.

The variation in the moisture content of the base material results in the alternation of the degree of saturation that ultimately impacts the pore water pressure or the suction properties of the materials (Dawson et al. 2000). The mechanical parameters of the materials may vary with changes in the suction properties. Many authors (e.g., Raad et al. 1992; Yuan and Nazarian 2003; Richter 2006; and Cary and Zapata 2010) studied the impact of the moisture content on the strength and stiffness of the base materials. The amount of moisture present in most granular materials has been found to influence the resilient response of the materials in both the laboratory and in-situ conditions. Lekarp et al. (2000) reported that the resilient modulus of the base material showed a drastic decrease as the saturation level reached to 100%. Similarly, Ekblad and Isacsson (2006) measured the resilient moduli of the coarse granular materials at various moisture contents up to saturation. The authors reported that the materials with high fines contents showed a significant reduction in their resilient moduli whereas the materials with less fines contents showed a minor reduction in their resilient moduli even when the moisture content increased up to saturation.

Base Material Characterization for Design and Construction

The variation of particle size in the mix contributes to the heterogeneous nature of the base, and the orientation of coarse particles contributes to the anisotropic behavior of the base. Although heterogeneity and anisotropy are simplified for pavement design purposes, the modelling and construction process of base course encounter many constraints posed by the fines content, material handling, contamination of material, methods use for construction, approaches for quality control and more.

Variation of Fines Content. The stability of the aggregate matrix of the base material depends on the amount of fines available to fill the void spaces (Ghabchi et al. 2013). The deficiency of the fines in the mix may result in an unstable matrix due to excessive movement of the coarse particles with respect to one other. Excessive fines may also result in an unstable matrix due to the replacement of the contact points of the granular materials by fines. In both of these scenarios, the materials exhibit a lower shear strength and resilient modulus resulting in a high permanent deformation. Several researchers have proposed the optimum fines contents (Gray 1962; and Tutumluer and Seyhan 2000) or optimum gradation (Brown and Chan 1996) in order to obtain the maximum strength. The optimum fines content depends on several factors like the type of coarse aggregates, the shape and size of the coarse aggregates, and the type of fines.

Improper Material Handling. Although it is possible to control the material gradation and moisture content in the laboratory, it is not possible to control these parameters accurately in the field during construction. Improper material handling may lead to aggregate segregation resulting in a non-uniform distribution of the fines in the aggregate mix. The aggregate segregation may contribute to the variation in the degree of compaction and may cause the reduction in the shear strength, stiffness and deformation resistance throughout the pavement sections.

Contamination of Unbound Aggregates. The contamination of the unbound aggregate layer during the pavement operation phase may influence the pavement performance. The migration of fines from the subgrade may contaminate the base. The possibility of the migration of the fines is exaggerated by a) high water table during the rainy seasons, b) the lack of separating layer between the base and subgrade, and c) the degrading subgrade or the use of a poor quality subgrade.

Variation in Methods of Compaction. The impact methods are typically used in the laboratory to compact the materials whereas the vibratory methods are adopted in the field to compact the layers of geomaterials. The mechanical responses of the granular materials after compaction may be different due to the differences in the compaction methods. Kaya et al. (2012) performed a comparative study between the impact and vibratory compaction methods on the unbound granular materials. The authors found that the impact method changed the gradations of the materials due to crushing and breakage of the particles. The change in the gradation of the materials resulted in an alteration of the optimum moisture content (OMC). The authors reported that higher California Bearing Ratio (CBR) were achieved for the materials compacted with the vibratory methods but higher resilient moduli were obtained for the materials compacted with the impact method.

Differences in Quality Control Approaches. One of the crucial steps in the construction of pavements is proper quality control and quality assurance to ensure the constructed pavements meet the design requirements. The Proctor tests are performed in the laboratory to attain the maximum density and the optimum degree of compaction, whereas the nuclear density tests are conducted in the field to estimate the density as a quality measure (White et al. 2006). In that scenario, a gap between the laboratory and field tests exists that may result in undesirable outcomes in the context of the quality control. Moreover, a clear relationship between the material performance in the laboratory and in the field is required to validate the test results obtained from the pavement construction sites.

Methodology for Characterizing Base Materials

The elasto-plastic behavior of the unbound aggregate bases affects the strength characteristics of that layer (Habiballah and Chazallon 2005; Huang et al. 2010). Although the stress-strain response of the bases for a short-term loading is linear, the responses for a long-term loading posed by a large number of repeated vehicle loads could be nonlinear. In other words, the design methods based on the elasticity of the materials cannot be relied for understanding the plastic strains accumulating in the granular layer of pavement systems.

A comprehensive review of the common test methods applied to the unbound granular materials for determining the pavement performance is provided in the NCHRP Project 4-23 by Saeed et al. (2001). During the early developmental period of the pavement design procedure, the soil strength

parameters such as the CBR value, Hveem R-value, and Soil Support Value (SSV) were used. These parameters were adopted with the assumption that the failure in the pavement occurred in the weakest pavement layers, i.e. the subgrade. However, the failure of the flexible pavement may occur due to the excessive rutting or cracking of the pavement layers, and the softening caused by the surface layer cracking (Brown and Chan 1996). The 1993 AASHTO pavement design guide recommended the use of the resilient modulus instead of the parameters such as CBR and SSV. The resilient modulus tests allow for the characterization and modeling of the elasto-plastic and the softening and hardening behaviors of the granular materials in the pavement materials.

In general, the strength and stiffness tests are conducted for characterizing the strength, modulus, and permanent deformation behaviors of the unbound aggregate materials in pavement systems. The strength and stiffness tests listed by Saeed et al. (2001) are provided in Table 2. Out of these tests, the triaxial tests are the most common strength tests and the resilient modulus tests are the most common stiffness tests.

Table 2.1. Tests for Unbound Granular Materials (from Saeed et al. 2001)

Property Measured	Test name
Shear Strength	Static Triaxial Shear
	Repeated Load Triaxial
	Unconfined Compression
	Direct Shear
	CBR
	Hveem Stabilometer
Stiffness	Resilient Modulus
	Resonant Column

Traditional Tests for Unbound Granular Materials

Out of many available tests for the unbound granular materials, three types of tests – unconfined compressive test, resilient modulus test and permanent deformation test, are discussed below.

Unconfined Compression Test. The unconfined compression tests are common methods to determine the unconfined compressive strength (UCS) of granular materials used in pavements (Schnaid et al. 2001; Piratheepan et al. 2010; Wen et al. 2010). TXDOT follows test procedure Tex-117-E for determining UCS of granular materials. The testing system consists of a loading frame with a crosshead mounted hydraulic actuator to measure applied load and induced deflection, and a data acquisition system (Figure 2.1a). A typical result of the unconfined compression test is shown in Figure 2.1b. The maximum stress experienced by the specimen (or the stress at failure of specimen) is the UCS.

Resilient Modulus Test and Permanent Deformation Test. One of laboratory methods advocated for determining these two parameters is the repeated load triaxial test as per AASHTO T-307. The testing system consists of a loading frame with a crosshead mounted hydraulic actuator (Figure 2.2a). A load cell is attached to the actuator to measure the applied load. The specimen is housed

in a triaxial cell where a confining pressure is applied. As the actuator applies the repeated load, specimen deformation is measured by a set of linear variable differential transducers (LVDTs) or noncontact sensors. A data acquisition system records all data during testing.

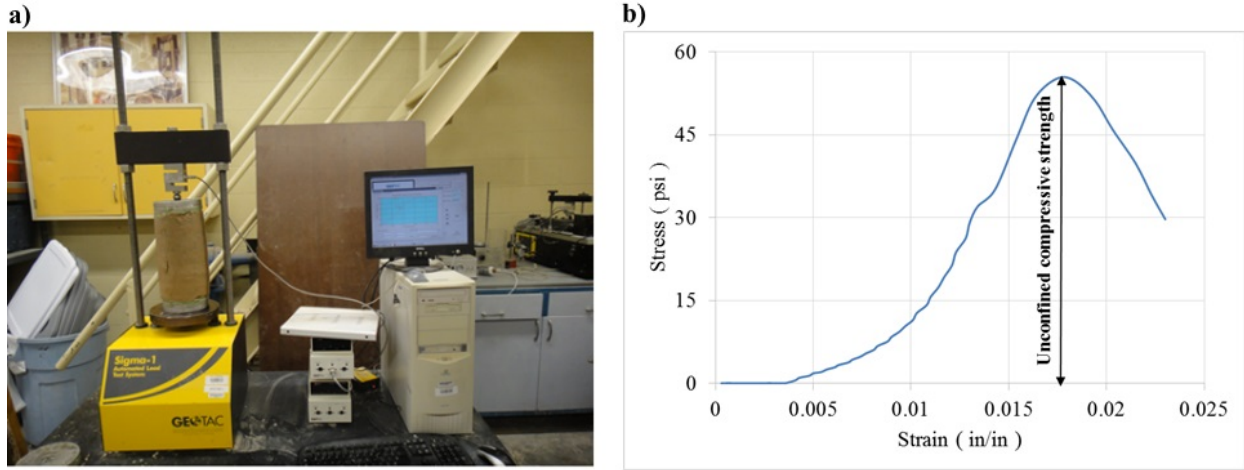


Figure 2.1 Unconfined compression test: a) Test setup and b) Typical output

The resilient modulus determined from the repeated load triaxial test is defined as the ratio of the repeated axial deviator stress to the recoverable or resilient axial strain:

$$M_r = \frac{\sigma_d}{\epsilon_r} \quad \text{Equation 2.1}$$

where M_r is the resilient modulus, $\sigma_d = (\sigma_1 - \sigma_3)$ is the deviator stress, and ϵ_r is the resilient (recoverable) strain in the vertical direction (see Figure 2.2b).

The load cycle duration is 1 second that includes a 0.1 second load duration and a 0.9 second rest period. The test is started by applying 1000 repetitions of a load equivalent to a maximum axial stress of 15 psi at a confining pressure of 15 psi. This is followed by a sequence of loadings with varying confining pressures and deviator stresses as tabulated in Table 2.2. These loading cycles are slightly modified from AASHTO T-307 in that the specimen is subjected to 25 repeated axial loads for each sequence instead of 100 cycles. A typical result obtained on a base material is shown in Figure 2.2c. Tutumluer (2013) provided a comprehensive review of the resilient modulus models for determining model parameters from the measured data. For example, the Mechanistic Empirical Pavement Design Guide (MEPDG) recommended the following relationship to compute the representative resilient modulus (M_R) of unbound aggregates and fine-grained soils.

$$M_R = K_1 p_a \left(\frac{\theta}{p_a} \right)^{K_2} \left(\frac{\tau_{oct}}{p_a} + 1 \right)^{K_3} \quad \text{Equation 2.2}$$

where θ is the bulk stress = $\sigma_1 + \sigma_2 + \sigma_3$, τ_{oct} is octahedral shear stress = $1/3[(\sigma_1 - \sigma_2)^2 + (\sigma_1 - \sigma_3)^2 + (\sigma_2 - \sigma_3)^2]^{1/2}$, p_a is atmospheric pressure, and K_1 , K_2 , and K_3 are constants obtained from experimental data.

The deformation responses of base due to the repeated applied loads contains resilient and plastic or non-recoverable deformations (Figure 2.2b). The measure of cumulative non-recoverable

deformations up to the end of the loading cycles, which provides the information about the plastic deformation of the base, is essential to understanding its rutting behavior. The conditioning phase of the resilient modulus test can be utilized for determining the permanent deformation of a specimen.

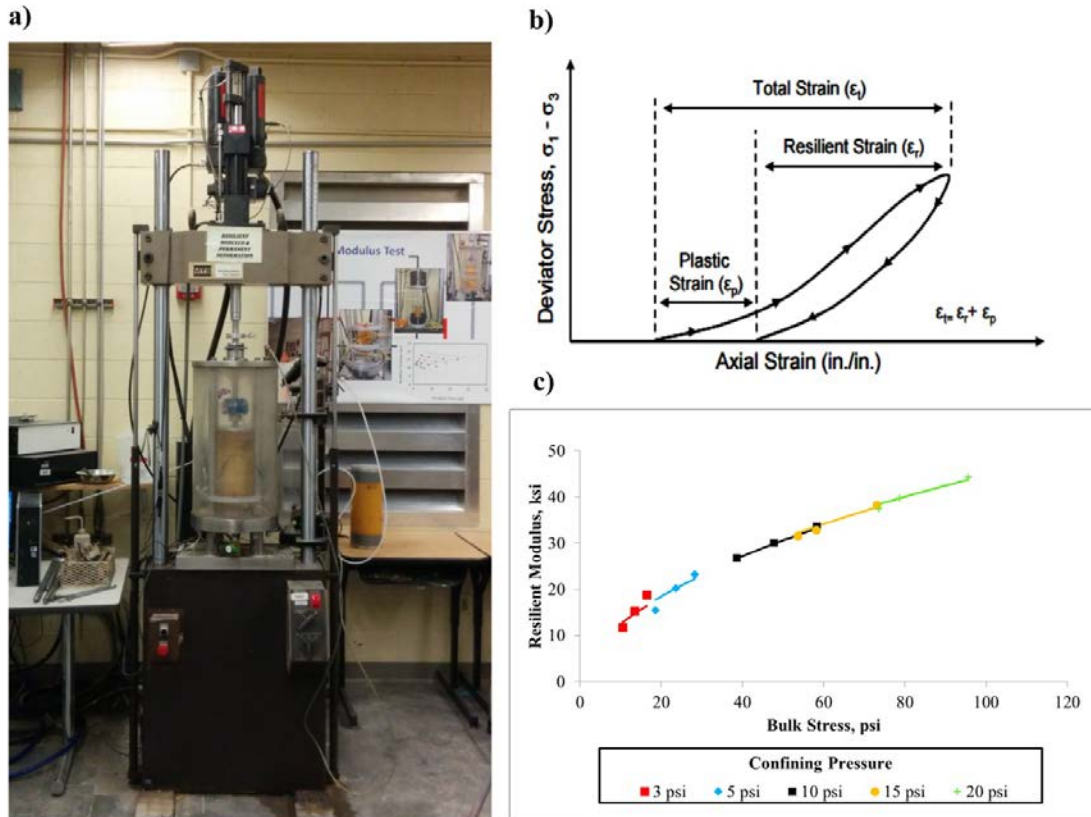


Figure 2.2 Resilient Modulus and Permanent Deformation Test: a) Test setup, b) Specimen response during Resilient Modulus Test (From Buchanan 2007) and c) Typical result obtained from Resilient Modulus Test

Nondestructive Tests for Unbound Granular Materials

The common nondestructive test methods of characterizing the base materials are the Free-Free Resonant Column (FFRC, Celaya et al. 2006; Williams and Nazarian 2007; Mazari et al. 2014), the Portable Seismic Property Analyzer (PSPA) and the Light Weight Deflectometer (LWD, Celaya et al. 2006; Von Quintus et al. 2009; Mazari et al. 2014).

Free-Free Resonant Column (FFRC) is currently based on Tex-148-E procedure. The FFRC test was originally developed for the concrete specimens (ASTM C215). The test was modified for base and subgrade materials through hardware and software modifications (Stokoe et al. 1994; Nazarian et al. 2003). The FFRC test uses an instrumented hammer as an impulse source for generating impulsive waves over a range of frequencies, an accelerometer to capture the generated waves, and a data acquisition and data processing system. The propagated waves have one or more resonating frequency(ies) that depends upon the dimensions and stiffness of the specimen. The resonant frequencies (longitudinal and possibly shear resonant frequencies) are identified. Figure

2.3 shows the FFRC test and the output of test in form of frequency response. The modulus (E) of the specimen is provided by (Richart et al. 1970):

$$E = \rho (2f_c L)^2 \quad \text{Equation 2.3}$$

where L is the length of the specimen, f_c is the fundamental mode frequency related to the specimen vibration and ρ is the mass-density of the specimen.

Table 2.2 Loading sequences for Resilient Modulus (MR) and Permanent Deformation (PD) Tests (From Gandara 2004)

Sequence	Confining Pressure		Contact Stress		Cyclic Stress		Maximum Stress		N _{rep}	Tests
	kPa	psi	kPa	psi	kPa	psi	kPa	psi		
Conditioning	103.5	15	10.4	1.5	93.1	13.5	103.5	15	1000	PD
1	20.7	3	2.1	0.3	18.6	2.7	20.7	3	25	MR
2					41.4	6	41.4	6		
3					62.1	9	62.1	9		
4	34.5	5	3.4	0.5	31.1	4.5	34.5	5	25	
5					69	10	69	10		
6					103.5	15	103.5	15		
7	69	10	6.9	1	62.1	9	69	10	25	
8					138	20	138	20		
9					207	30	207	30		
10	103.5	15	10.3	1.5	58.6	8.5	69	10	25	
11					103.5	15	103.5	15		
12					207	30	207	30		
13	138	20	13.8	2	89.7	13	103.5	15	25	
14					138	20	138	20		
15					276	40	276	40		

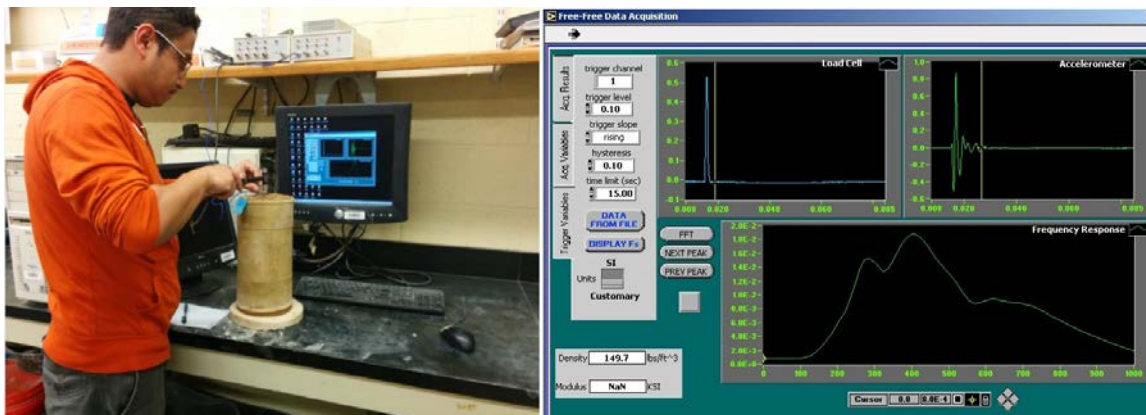


Figure 2.3 The FFRC test (left) and output of the test (right)

Portable Seismic Property Analyzer (PSPA) consists of two accelerometers and a source packaged into a hand-portable system (Figure 2.4). The source produces an impulsive impact on the material surface that generates stress waves. The signals of the stress waves are captured by two accelerometers. The fast Fourier analysis of the signals are performed to compute the average shear wave velocity (V_s) of the material with an appropriately assumed Poisson's ratio. The low-strain or linear elastic modulus (E) (also termed as a seismic modulus; Nazarian et al. 2003) of a layer is, then, derived with the Poisson's ratio (ν) and mass-density(ρ) of the material using following equation:

$$E=2 \rho V_s^2 (1+ \nu)$$

Equation 2.4

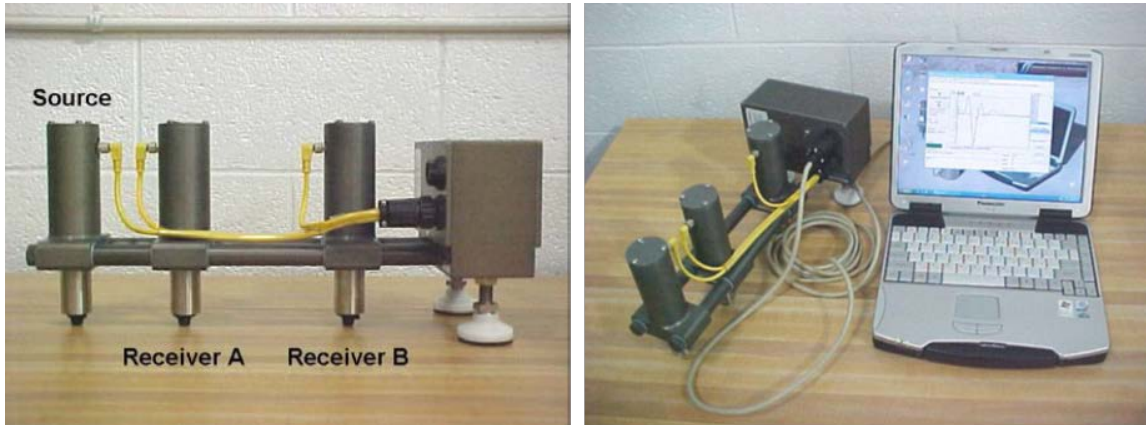


Figure 2.4 Portable Seismic Property Analyzer

Light Weight Deflectometer (LWD) is a portable device (Figure 2.5) that measures the surface deflection under a given load and computes an effective modulus of a pavement system. The LWD test assumes that the material is a single elastic layer. The effective modulus, E_{eff} , is computed from

$$E_{eff}= [(1- \nu^2) F/ (\pi a d_{LWD})] f$$

Equation 2.5

where ν = Poisson's ratio of geomaterial, a = radius of load plate, F = LWD load, d_{LWD} = LWD surface deflection, and f = shape factor which is a function of the plate rigidity and soil type.

Performance Tests for Unbound Granular Materials

To understand the behavior of the geomaterials, various performance tests are used. The plate load test has been used by many investigators (e.g., Sweere 1990; DeMerchant et al. 2002; Alshibli et al. 2005; and Li and Baus 2005) to understand the load-deformation characteristics of the geomaterials. The schematic of the plate load test apparatus is shown in Figure 2.6. The plate load test set up consists of a hydraulic actuator mounted on a heavy truck to apply load, a load cell to measure the load, a steel plate to impose the load on the road surface and one or more LVDTs to measure the vertical displacements. The concept of stiffness measurement is based on determining the ratio of the applied load and measured deformation under the plate. As the deformations are related to the combined effects of multiple layers below the plate, this type of in situ tests offers opportunities to measure a combined stiffness of the target pavement layer (the layer on which plate load test is conducted) and other layer below them. However, one of the drawbacks of the plate load test is that the deformations of individual layers cannot be measured quantitatively.

Alshibli et al. (2005) used the plate load test on compacted layers of base and subgrade to measure their stiffness characteristics and correlate them with the measured stiffness from other devices such as the Geogauge, Light Weight Deflectometer and Dynamic Cone Penetrometer. The authors conducted tests at the Louisiana Transportation Research Center (LTRC) laboratory on a test box that measured 5 ft long, 3 ft wide and 3 ft deep. The test box consisted of a 12-in. thick subgrade layer and a 16-in. thick base. The plate load tests were performed according to the ASTM D1195-93. The authors reported good statistical correlations between the modulus from the plate load test and the corresponding moduli from the other devices.



Figure 2.5 Light Weight Deflectometer

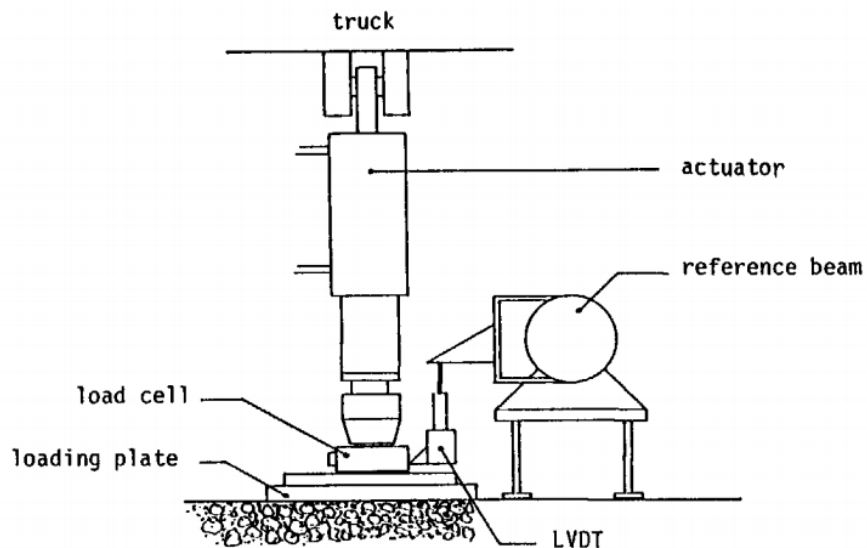


Figure 2.6 Principle of Plate Load Test Apparatus (from Sweere 1990)

Previous Studies at UTEP

The geomaterial testing facility at the Center for Transportation Infrastructure Systems (CTIS) at The University of Texas at El Paso (UTEP) has a 300-kip Material Testing and Simulation (MTS) system that is used for characterizing geomaterials under different load magnitudes and frequencies. Gandara and Nazarian (2006), Amiri et al. (2009), Gautam et al. (2009) and Mazari et al. (2014) conducted plate load tests at UTEP to measure the performance of pavement systems with large (36 inch in diameter) specimens. The wall of the tank is made with 1-in. thick polyethylene, and the height of the tank is 28 in.

Gandara and Nazarian (2006) performed a series of load-deformation tests on large specimens prepared with three different base materials. A 6-in. thick base layer was prepared at the OMC over a 14-in. thick subgrade layer. The tests were performed on the specimens after construction, after the saturation of the subgrade and after the saturation of the base and subgrade. Up to 2000 haversine pulse loads with the durations of 0.1 sec followed by 0.9 sec of rest periods were applied to the specimens. The magnitude of the peak load was 2000 lb with a seating load of 200 lb. The resilient deformation of the base layer was computed at the end of the 200th cycle and the permanent deformation after the last cycle. In addition to those experiments, a series of numerical simulation with VESYS model was performed to obtain the theoretical deformations. It was found that the average deformation of the base when the base and subgrade were saturated was 10 times more than the condition when the base and subgrade were placed at the OMC. It was also noted that the predicted deformations from the numerical models and the measured deformations from the laboratory experiments did not favorably match.

Amiri et al. (2009) studied the performance of one base placed over two different types of subgrade. The authors conducted numerical simulations, as well as small-scale tests and full-scale tests with the same materials. A 5-in. thick layer of base was prepared on top of the subgrades for the small-scale tests. For full-scale tests, a 10-in. thick base layer was compacted in a road section with the same materials used in the small-scale tests. The vertical dimension of the full-scale test model was twice the small-scale tests. Moisture content of the specimens were varied as discussed in Gandara and Nazarian (2006). The numerical simulations were conducted with finite element models of the base, subgrade and the tank body using ABAQUS. In the case of the small-scale tests, a cyclic ramp load at a rate of 500 lb/min. was applied to the specimens. The ramp load was increased in such a way that the peak loads varied from 500 lb to 5000 lb. In the case of the full-scale tests, plate load tests with 6.6 in. diameter plates were carried at different road sections. The load tests were carried out with a continuous loading pattern, and the peak load was 30 kips. The load-deformation characteristics measured from the small-scale and full-scale tests were similar. The authors also reported that the responses from the numerical simulation were similar to the experimental results after applying appropriate transfer functions.

Gautam et al. (2009) studied the mechanical properties of five different base materials. The authors prepared guidelines and test protocols to use locally available materials, not meeting the material specification of TXDOT, by adding chemical additives or modified gradation for construction of low-volume roads. Small-scale tests were one type of tests conducted to measure the field performances of bases at various moisture levels. A 6-in. thick base layer was prepared over a subgrade in the tank. The moisture contents of the materials were varied as discussed in Gandara and Nazarian (2006). Two types of loading, cyclic ramp and sinusoidal, were applied to the

specimens. In the case of the cyclic ramp loading, loads were applied at a rate of 500 lb/min. as mentioned by Amiri et al. (2009). The peak load was varied from 700 lb to 11000 lb. The loads in the case of the sinusoidal loading were applied with an amplitude of 2000 lbs and a frequency of 1 Hz. The corresponding deflections were measured in both loadings for the treated and non-treated bases. The authors observed that the permanent and resilient deformations of the treated bases were less than non-treated base and concluded that the use of the additives on the locally available materials could be a viable option for a better-performing pavement.

Mazari et al. (2014) performed several small-scale tests to compare the numerical and experimental responses of pavements using different loads, loading areas and moisture conditions. The pavement performance related parameters such as the deformation of the pavement layers were predicted after analyzing the results of the resilient modulus tests and the numerical models. The authors used one granular base and four kinds of fine-grained soils. Each specimen had a layer of 6-in. thick geotextile over the subgrade. The cyclic plate loads with nominal contact stresses of 30 psi to 90 psi were applied to the specimens, and the corresponding deformations were measured. To perform the numerical simulations, the authors adopted finite element models of the geotextiles and applied circular loads similar to the small-scale tests. The authors found the deflections of the geotextiles of various specimens were comparable to the deflections predicted by the numerical models with proper transfer functions.

Chapter 3 – Research Approach and Testing Procedure

Previous research has shown that the amount of fines content and moisture content present in the material affect the performance of the pavement systems. However, the allowable amount of fines for base materials is not strictly specified. In spite of implementation of a strict material specification for pavement construction, the gradation of material could change due to various reasons such as improper material handling, contamination of base material by subgrade. Similarly, the moisture content of a base material may alter during pavement construction and operation by exposure to excessive water and percolation of rainwater from pavement surface. To understand the effect of fines content and moisture content, 12 different series of tests were performed at four different fines contents and three different moisture contents as tabulated in Table 3.1. The nominal fines contents of 5% to 20% were used. The amount of moisture in the base materials was varied by OMC, OMC-1% and OMC+1% to capture the behavior of base materials at optimum, dry and wet conditions.

Table 3.1 Overall tests of base materials at different fines contents and moisture contents

Test No.	Nominal Fines Content (% by weight)	Nominal Moisture Content (% by weight)
1	5	OMC-1
2		OMC
3		OMC+1
4	10	OMC-1
5		OMC
6		OMC+1
7	15	OMC-1
8		OMC
8		OMC+1
10	20	OMC-1
11		OMC
12		OMC+1

Materials for Tests

A local producer provided a ready-to-deliver base material for this research. The material met the gradation specification for TxDOT Grade 1 (high quality) base. As shown in Figure 3.1, the base material contained about 2% fines. An additional material that primarily contained fines was also received from the same source.

Cooper et al. (1985) provided a relationship for maintaining the structural stability of a granular material when the percentage of fines is changed. Cooper et al.'s relationship, which was used in this study, is in the form of

$$P = \frac{(100-F)(d^n - 0.075^n)}{(d^n - 0.075^n)} + F \quad \text{Equation 3.1}$$

where P = percentage passing a sieve of size d in mm, F = percentage of material passing through a 0.075 mm sieve (i.e., fines content), d = sieve size (mm), D = maximum particle size (mm), and n = power relationship (typically 0.45). The gradations for the four different bases formulated using Equation 3.1 are shown in Figure 3.1 and Table 3.2. Soil classifications of these bases as per AASHTO and USCS and their OMCs and maximum dry densities for bases with different fines contents are tabulated in Table 3.3.

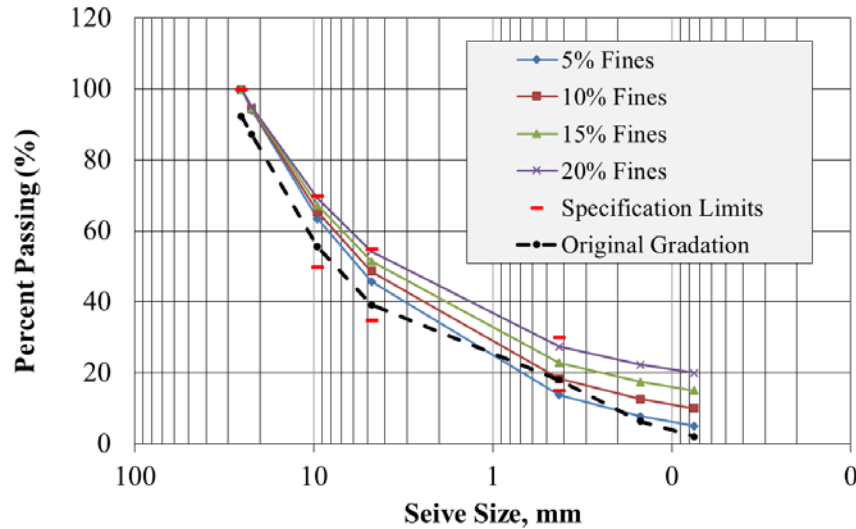


Figure 3.1. Particle size distribution for material mixes of different fines contents

Table 3.2. Particle size distribution of mixes

Standard Sieve Size	Nominal Sieve Opening (mm)	(% Passing)						
		Acceptance Limits		Original Gradation	5%	10%	15%	20%
		Low	High					
1"	25.4	100	100	92.3	100.0	100.0	100.0	100.0
7/8"	22.22	65	90	87.2	94.0	94.3	94.7	95.0
3/8"	9.52	50	70	55.6	63.4	65.4	67.3	69.2
#4	4.75	35	55	39.2	45.7	48.6	51.4	54.3
#40	0.42	15	30	17.9	13.8	18.3	22.9	27.4
#100	0.15	-	-	6.4	7.7	12.6	17.4	22.3
#200	0.075	-	-	2.0	5.0	10.0	15.0	20.0

Table 3.3 Soil classifications for base materials

Material	Atterberg Limits		Proctor Tests		Classification	
	LL	PI	OMC, %	MDD, pcf	AASHTO	USCS
Original	22	10	--	--	A-2-4(0)	GW
5% Fines	23	10	6.3	145	A-2-4(0)	GW-GC
10% Fines	24	9	6.4	144	A-2-4(0)	GP-GC
15% Fines	26	9	7.2	142	A-2-4(0)	SC
20% Fines	28	9	7.2	139	A-2-4(0)	SC

Test Procedure

Moisture-Density and Moisture-Modulus Relationships

The maximum dry density (MDD) and optimum moisture content (OMC) were determined for each of the four mixes as per Tex-113-E. The results are shown in Figure 3.2 and summarized in Table 3.3. The MDD decreases and the OMC increases with the increase in fines content. The specimens used to determine the moisture-density relationship were also used to determine the seismic modulus with FFRC tests. A typical relationship between moisture vs density and moisture vs modulus for the mix of 20% fines content is shown in Figure 3.3. Although maximum dry density occurs at optimum moisture content, the maximum Young's modulus occurs at the moisture content less than OMC. In other words, the modulus at the OMC is less than the maximum modulus.

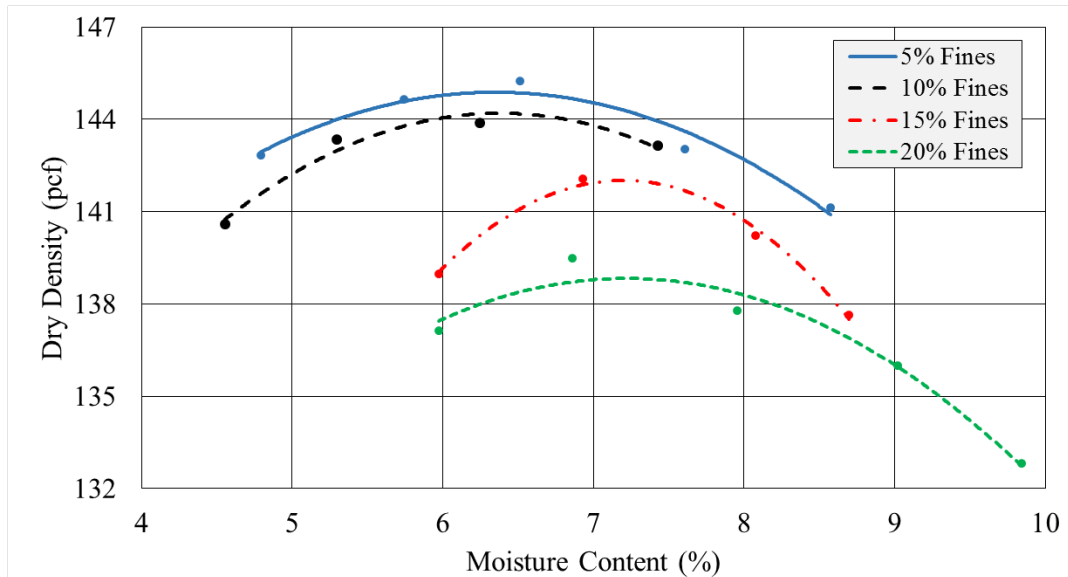


Figure 3.2 Moisture-density relationships for bases various fines contents

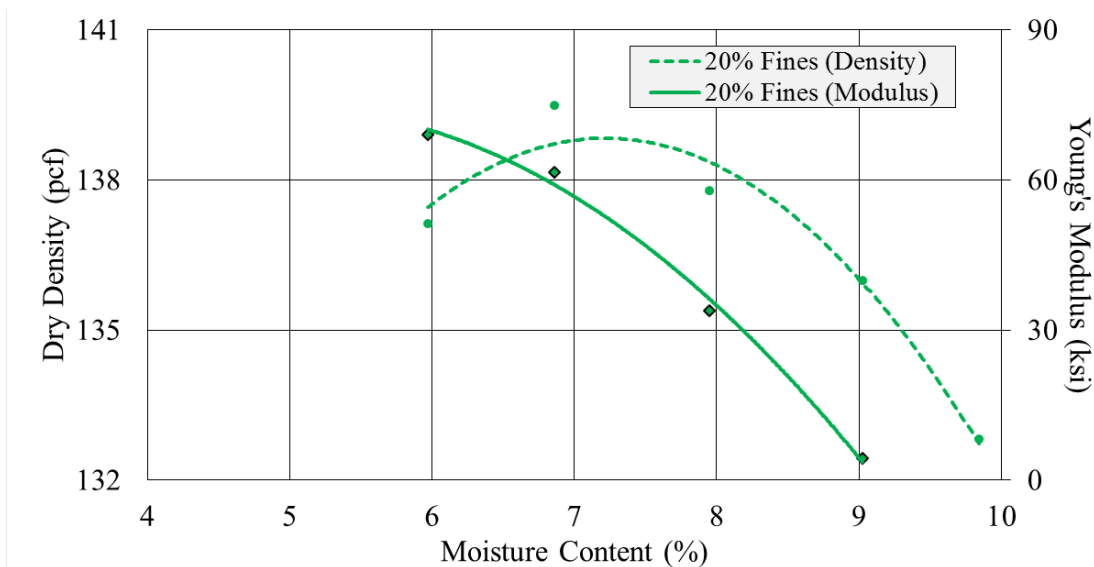


Figure 3.3 Typical moisture-density and moisture-modulus relationships

Laboratory Mechanical Properties Tests

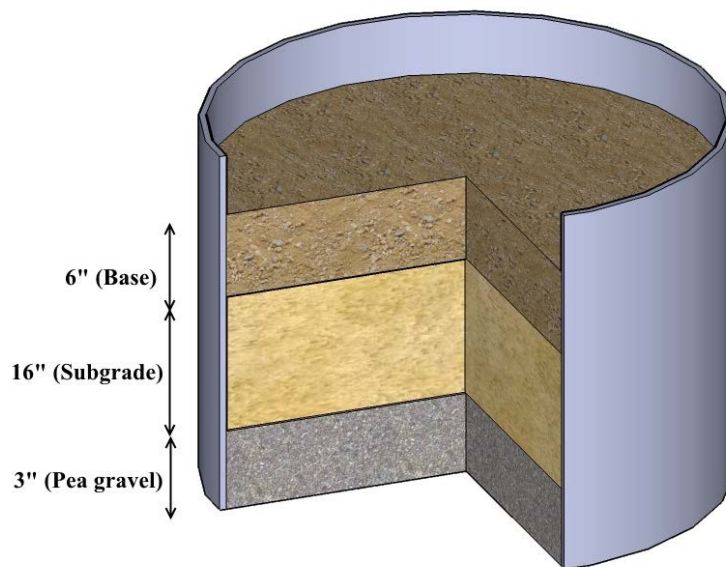
Aside from index tests as discussed above, the laboratory tests consist of the strength tests and stiffness tests. The strength tests consisted of the unconfined compression tests. The stiffness tests included the FFRC, permanent deformation and resilient modulus tests, as discussed in Chapter 2. To perform these laboratory tests, four cylindrical specimens were prepared for a specified fines content and moisture content, and tested about 24 hours after compaction. After completion of each test, the actual moisture content of the material was measured by breaking the specimen and drying it in the oven.

Small-Scale Test

Small-scale tests, as a substitute for controlled field tests, were carried out for each fines content and moisture content as mentioned in Table 3.1. The test tank and the loading system used by previous researchers at UTEP (Gandara and Nazarian 2006, Amiri et al. 2009, Gautam et al. 2009 and Mazari et al. 2014) were adapted for the small-scale tests.

The schematic of the tank with the layers of geomaterials for a small-scale test is shown in Figure 3.4. The test tank was made from a polyethylene sewage pipe with one closed end. The tank had an inner diameter of 36 in., height of 28 in. and thickness of 1 in. The bottom and the inner wall of the tank were lined with 6-mil thick polyethylene sheet. The soil profile for each specimen consisted of 3 in. of pea gravel at the bottom, 16 in. of subgrade over the layer of pea gravel and 6 in. of base over the subgrade as shown in Figure 3.4.

The subgrade and the configuration of layers were adopted from Mazari et al. (2014). The subgrade material was designated as SM material as per USCS soil classification. The MDD and OMC of the subgrade were 112 pcf and 15.2%, respectively. The subgrade layer was compacted in 2 in. lifts. Plate load tests as well as LWD and PSPA tests were conducted on each specimen 24 hours after the preparation of the base layer.



Note: Dimension not in scale

Figure 3.4 Schematic for tank cross-section for a small-scale test

The plate load test can be divided into two categories: a) Cyclic modulus test and b) Cyclic stage test. Both tests were conducted with an MTS system. The cyclic modulus tests were conducted with three different plates with diameters of 4 in., 8 in. and 12 in. (Figure 3.5). Haversine loads with peak contact pressures of 30 psi, 50 psi, 70 psi and 90 psi were applied on the tank using the different plates. Ten load pulses with loading and resting periods of 0.1 sec and 0.9 sec, respectively, were applied for each test regime. The typical applied loads and corresponding plate deformations from cyclic modulus test are shown in Figure 3.6. For each set of load, the modulus (termed as a cyclic modulus) of the material was computed using the average vertical stress and the average recoverable strain.

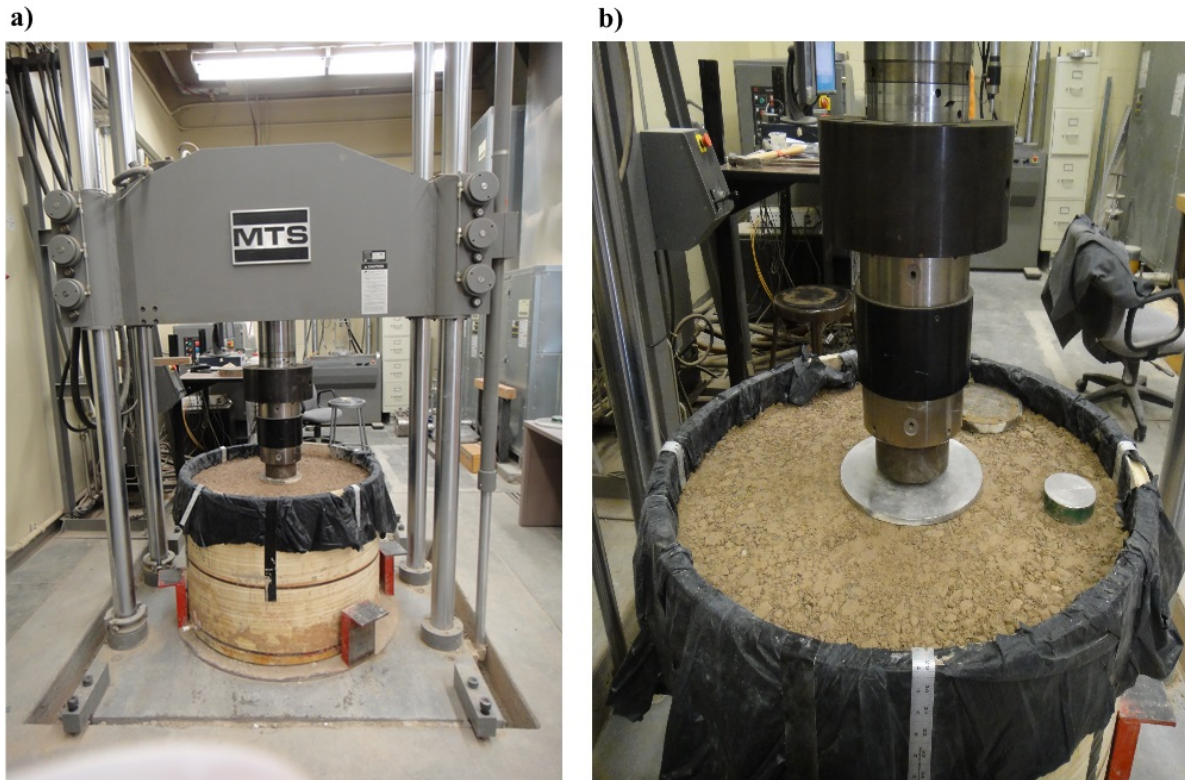


Figure 3.5 Small-scale test with a MTS system- a) Plate load test, and b) Three different plates for plate load tests

The cyclic stage tests were conducted after the cyclic modulus tests by using only the 8 in. plate. Two different loading patterns, cyclic ramp load and continuous load, were used for these tests. The loading rate for both loading patterns was 500 lb/min. In the case of the cyclic ramp load, the peak load was increased from 500 lb to 5000 lb in 500 lb increments. After reaching each peak load, the specimen was unloaded at an unloading rate of 500 lb/min, and allowed to rest for one minute before starting the next load. In the case of the continuous load, the load increased continuously from 0 lb up to 5000 lb, and unloaded in one minute. The typical load-deformation response of cyclic stage tests are shown in Figure 3.7. The outcomes of the cyclic stage test were i) load-deformation responses of cyclic ramp load and continuous load, ii) permanent deformation of material under the continuous load, and iii) stiffness of material measured from maximum load and corresponding deformation from the continuous load.

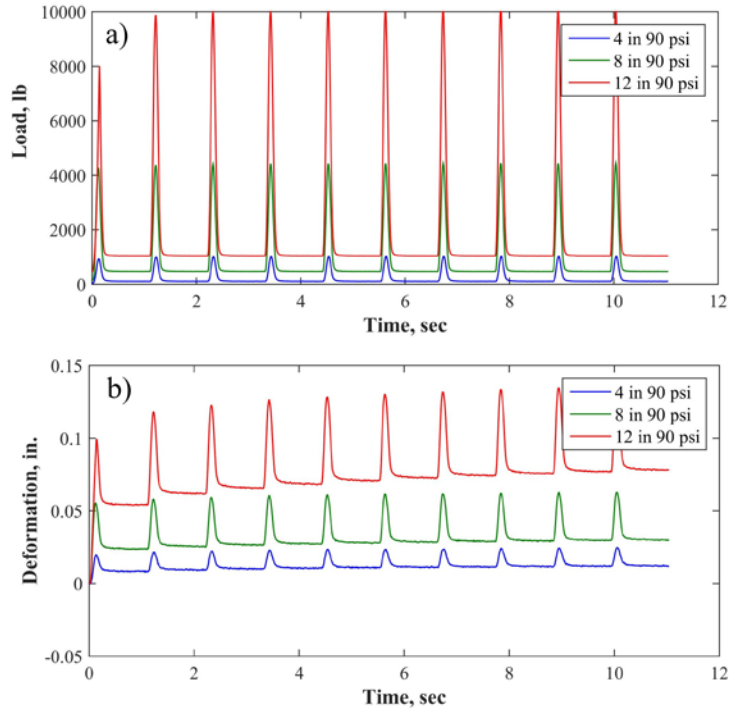


Figure 3.6 Typical load-deformation responses from the cyclic-modulus test: a) applied loads and b) measured deformations

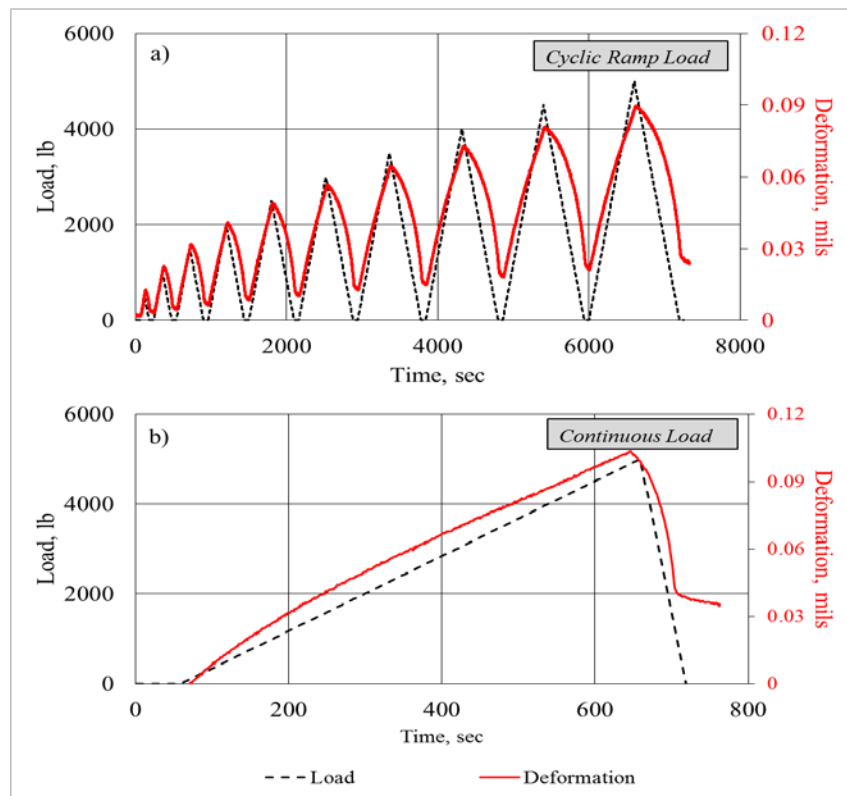


Figure 3.7 Typical load-deformation responses from the cyclic-stage test for a) cyclic ramp load and b) continuous load

An LWD manufactured by Zorn Instruments was adopted. The LWD tests were performed as per ASTM E2583. The effective modulus (termed as a LWD modulus) given in Equation 2.2 was computed assuming a Poisson's ratio of 0.4, the radius of load plate as 4 in., LWD load as 1700 lb, and shape factor of 2. For each specimen, three spots were chosen to conduct the LWD tests and measure deflections under the load plate (Figure 3.8).

The PSPA tests were conducted to measure seismic modulus (termed as PSPA modulus) at 24 different locations of tank surface as shown in Figure 3.9.



Figure 3.8 Small-scale test with LWD

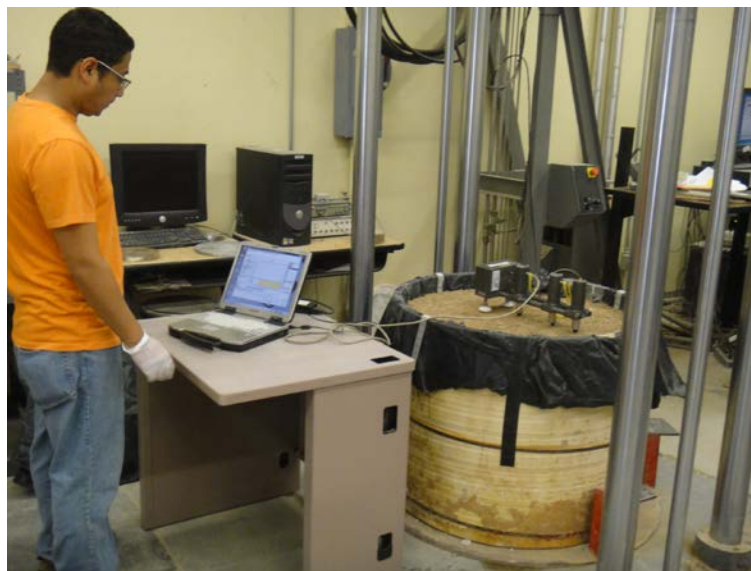


Figure 3.9 Small-scale test with PSPA

Chapter 4 – Results from Laboratory and Small-Scale Tests

This chapter presents the results from the laboratory tests on standard (6 in. in diameter and 12 in. in height) specimens and small-scale tests on large (36 in. in diameter and 6 in. in height) specimens. Twelve different tests sequences (see Table 3.1) were performed with a combination of moisture contents (OMC-1%, OMC and OMC+1%) and fines contents (5%, 10%, 15% and 20%).

Laboratory Tests

Four standard specimens were used for performing each of the laboratory tests, as discussed in Chapter 3. The first two specimens were used for conducting FFRC and unconfined compression tests and the other two specimens were used for conducting permanent deformation and resilient modulus tests. The results of these tests are presented in the following subsections.

Unconfined Compression Tests

The unconfined compressive strength (UCS) of standard specimens from unconfined compression tests are presented in Figure 4.1. Figure 4.1a shows the variations in strengths at different moisture contents for a specific fines content, i.e., the results grouped by fines content. Similarly, Figure 4.1b shows the results grouped by moisture content. The UCS decreases with increase in moisture

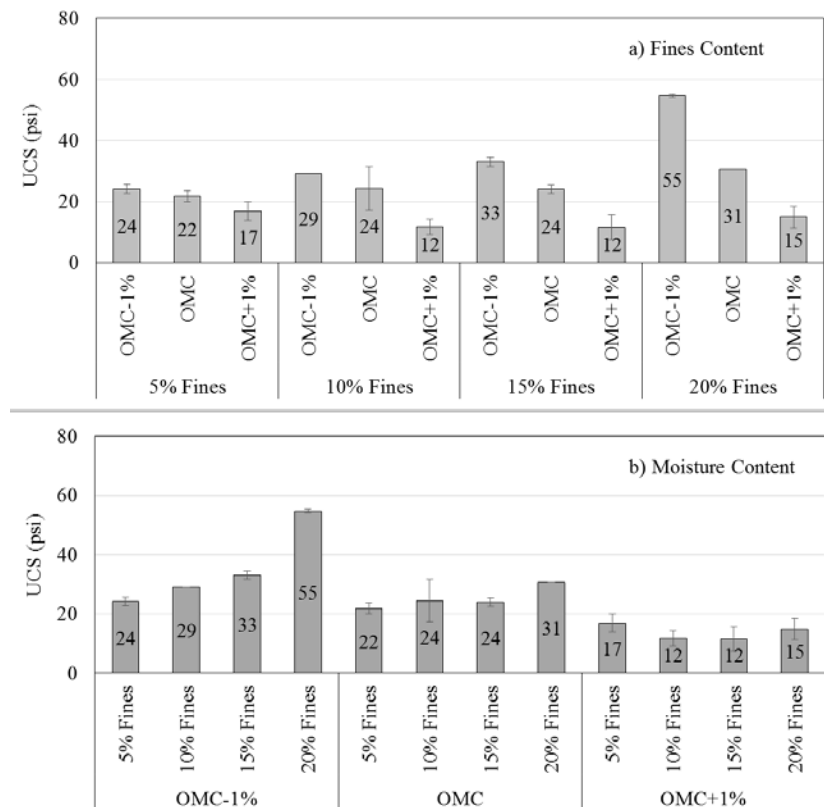


Figure 4.1. Unconfined compressive strength (USC) of standard specimens: a) grouped by fines content and b) grouped by moisture content

content. The results in Figure 4.1a also imply that the rate of reduction in strength increases with increase in fines content. In other words, for each fines content, the highest UCS occurs at OMC-1%. Figure 4.1b shows that the UCS increases with fines content when the nominal moisture content is either OMC-1% or OMC. The strengths for the OMC+1% specimens are less impacted by the variation in fines content.

FFRC Tests

Figure 4.2 shows the variations in the FFRC modulus of standard specimens with fines content and moisture content. As shown in Figure 4.2a, the FFRC modulus decreases with increase in moisture content for all fines contents. The results also show that a significant reduction in the FFRC modulus occurs for the specimens prepared with 15% fines content, especially between the moisture contents of OMC-1% and OMC. Figure 4.1b shows that the moduli for specimens prepared at OMC-1% are greater than the moduli at OMC and OMC+1%. In addition, the maximum moduli are achieved between 10% to 15% fines contents for all moisture contents.

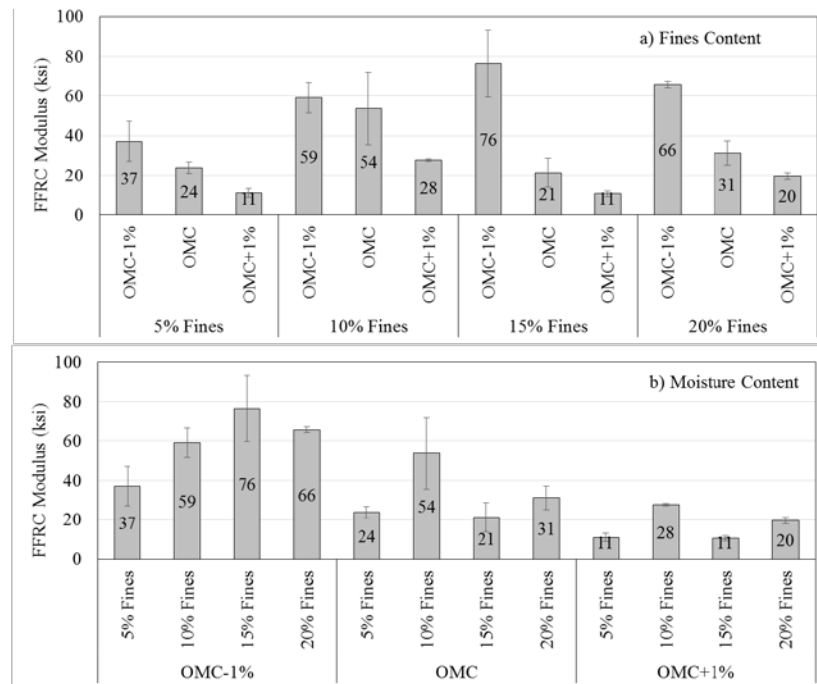


Figure 4.2 FFRC modulus of standard specimens: a) grouped by fines content and b) grouped by moisture content

Permanent Deformation Tests

Figure 4.3 shows the variations in permanent strains of standard specimens with the number of loading cycles. The resilient (permanent strain after 200 cycle) and permanent strains after the last cycle are summarized in Figure 4.4. The results for specimens prepared at OMC+1% are not available because the specimens were too wet to withstand the loads during the tests. The increase in the moisture content results in an increase in the resilient and permanent deformations, and hence resilient and permanent strains. As the fines content increases from 10% to 20%, the permanent strain typically decreases at OMC-1% and OMC. It is also observed that the specimens prepared with 10% fines content show more permanent deformation at OMC-1% and OMC as compared to the specimens prepared with other fines contents.

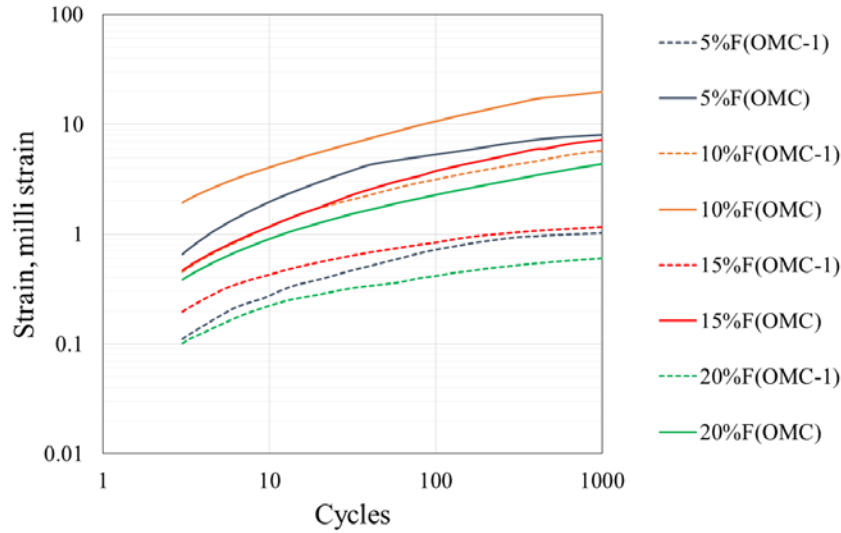


Figure 4.3. Strains measured at different loading cycles on standard specimens in permanent deformation tests

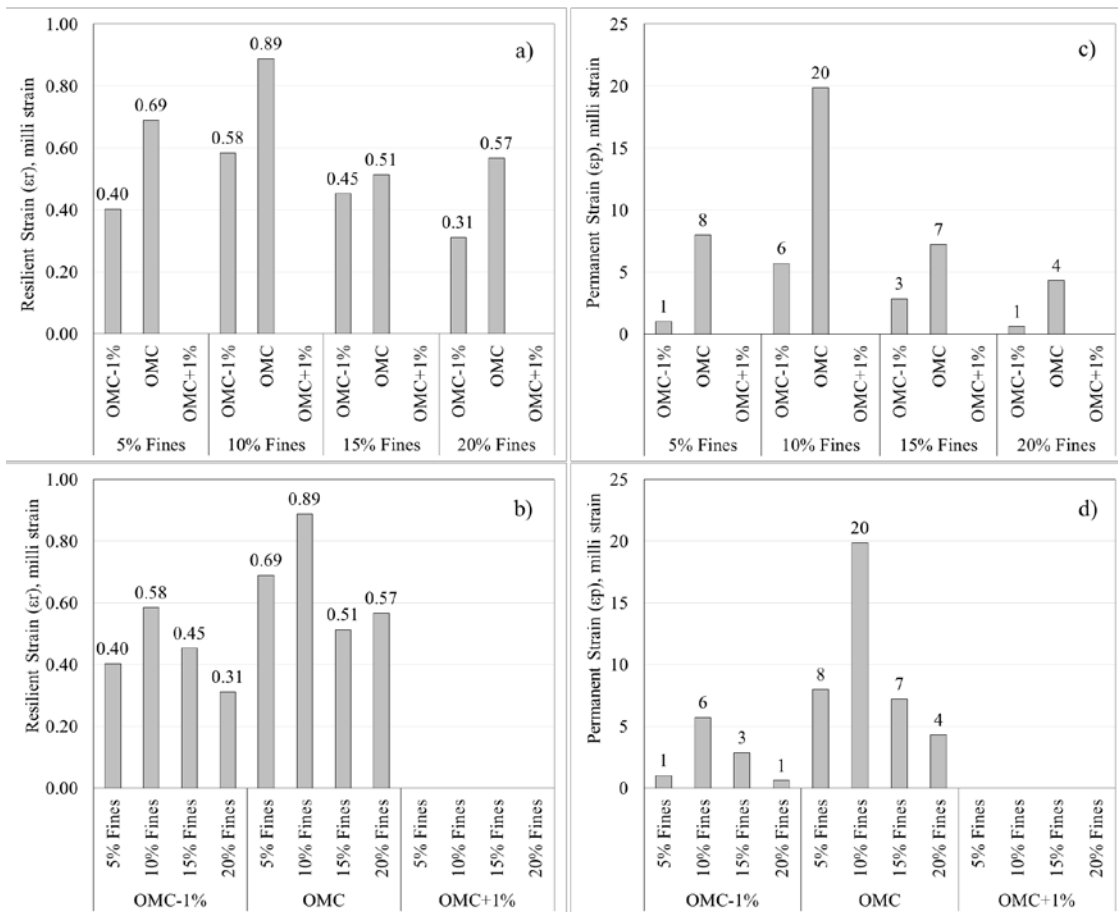


Figure 4.4 Resilient strains of standard specimens: a) grouped by fines content and b) grouped by moisture content. Permanent strains: c) grouped by fines content and d) grouped by moisture content.

Resilient Modulus Tests

The representative resilient moduli of specimens are presented in Figure 4.5. The results for the specimens prepared at OMC+1% are not available because the specimens were too wet to withstand the loads during the tests. The representative resilient modulus is computed using the bulk stress of 31 psi and the octahedral shear stress of 7.5 psi in Equation 2.2. The resilient moduli of specimens slightly decrease with increase in moisture content for all fines contents. From Figure 4.5b, the resilient modulus is not considerably influenced by the change in fines content at OMC-1% and OMC.

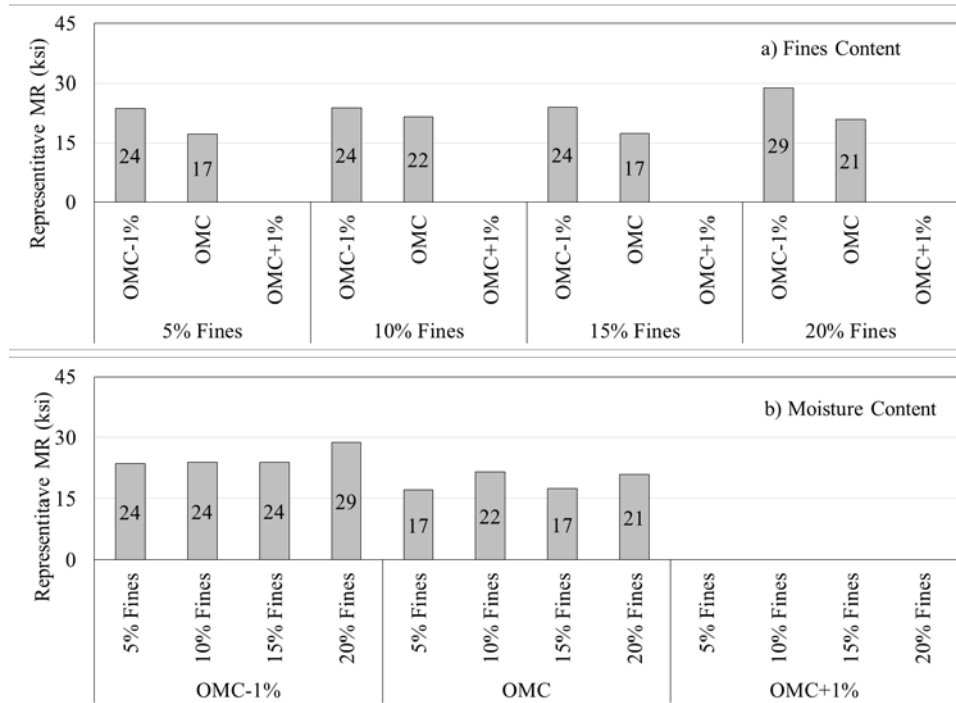


Figure 4.5 Representative resilient modulus (MR) of standard specimens: a) grouped by fines content and b) grouped by moisture content

Small-Scale Tests

One large specimen was used for performing each of the small-scale tests, as discussed in Chapter 3. The results of the tests are presented in the following subsections.

PSPA Tests

Figure 4.6 shows the variations in the PSPA modulus of the base on large specimens with fines content and moisture content. The PSPA moduli for the specimens prepared at OMC+1% are not reported because the specimens were too wet and too soft to couple seismic energy. Figure 4.6a shows that the PSPA modulus decreases with increase in moisture content. The results also show that the PSPA moduli of the specimens prepared with 15% fines content decrease more as compared to the other specimens when the moisture content increases from OMC-1% to OMC. The trends in Figure 4.6a for specimens prepared from 5% to 15% fines contents are similar to those for the FFRC tests. From Figure 4.6b, the PSPA modulus generally increases with increase

in fines content from 5% to 15% for the specimens prepared at OMC-1%. The results also show that the maximum moduli are typically achieved between 10% to 15% fines contents.

Figure 4.7 shows the PSPA modulus on top of the subgrade for each specimen before constructing the base layer. The modulus of subgrade varied from 24 ksi to 35 ksi throughout the tests with an average modulus of 28 ksi and a COV of 10%. This result shows that the mechanical properties of the subgrade for different specimens were similar throughout the tests.

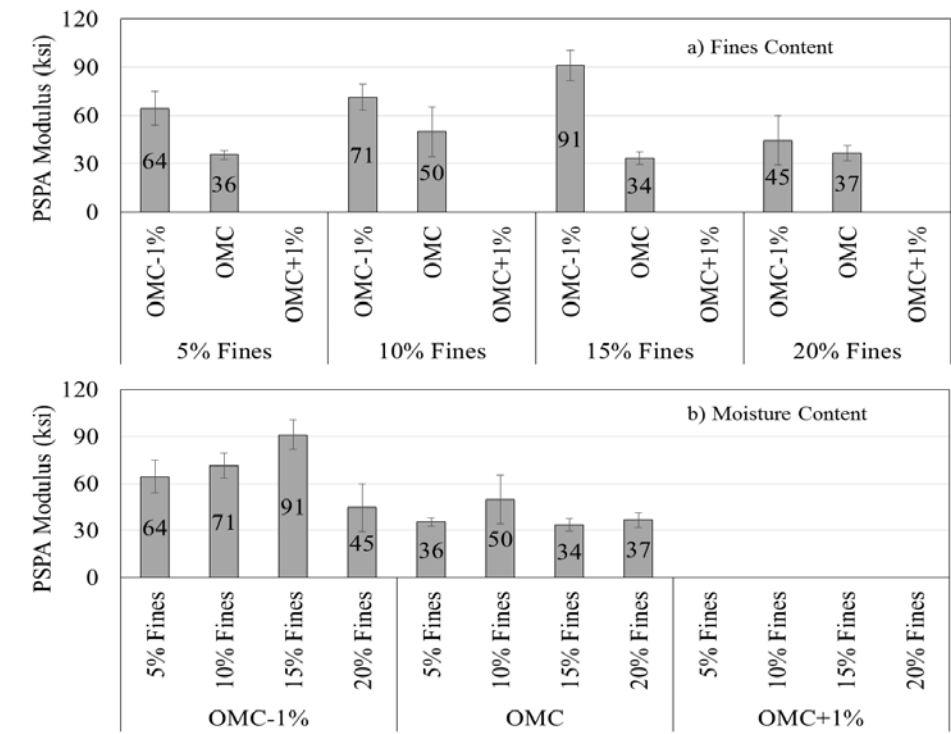


Figure 4.6 PSPA modulus of large specimens: a) grouped by fines content and b) grouped by moisture content

LWD Tests

Figure 4.8 shows the variations in the LWD modulus of base on large specimens with fines content and moisture content. The LWD modulus typically decreases with increase in moisture content (Figure 4.8a). These results also show that the rate of reduction in the modulus is higher for the specimens prepared with 10% and 15% fines contents as compared to the specimens prepared with 5% and 20% fines contents. Figure 4.8b shows that the LWD moduli for specimens prepared at OMC-1% are greater than the moduli at OMC and OMC+1%. The maximum moduli of the specimens are typically achieved with 10% fines content at OMC-1% and OMC. It should also be noted that the presented results with LWD are influenced by the modulus parameters of the subgrade layer because the thickness of base layer is only 6 in.

Figure 4.9 shows the LWD modulus on top of subgrade for each specimen before constructing the base layer. The modulus of subgrade varied from 4 ksi to 6 ksi throughout the tests with an average modulus of 5 ksi and a COV of 15%. This result shows that the mechanical properties of the subgrade for different specimens measured with the LWD tests were similar throughout the tests.

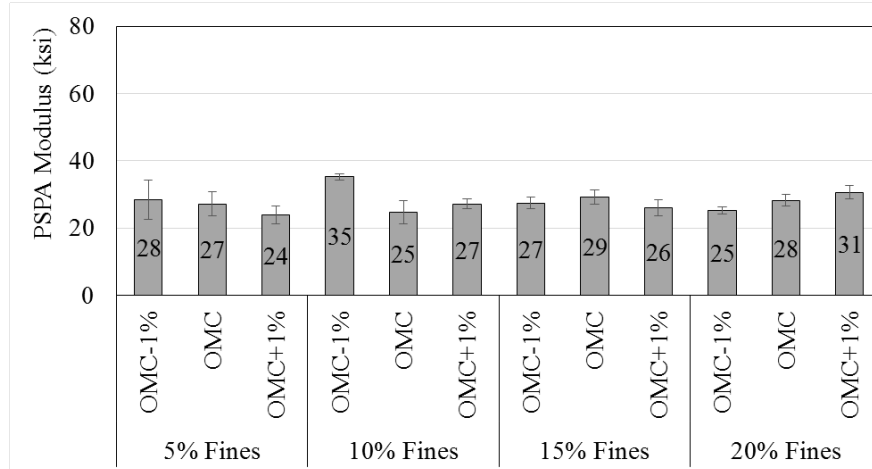


Figure 4.7 PSPA modulus of subgrade

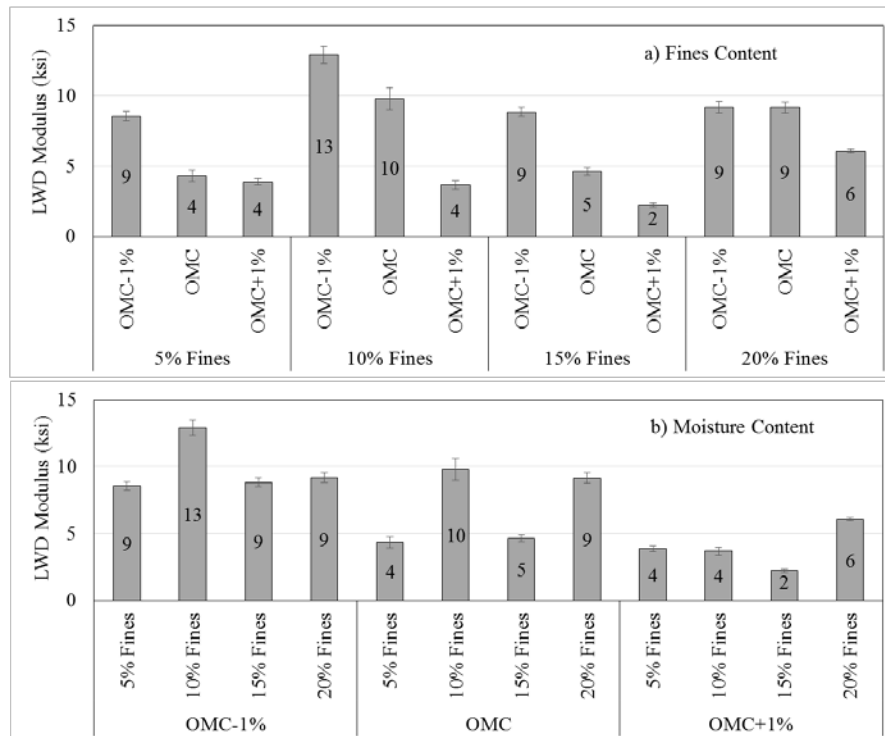


Figure 4.8 LWD modulus of large specimens: a) grouped by fines content and b) grouped by moisture content

Cyclic Modulus Tests

Figure 4.10 through Figure 4.12 show the variations in the cyclic modulus (i.e., the ratio of the measured average vertical stress and the average recoverable strain in a cyclic modulus test as discussed in Chapter 3) of base on large specimens with fines content and moisture content. These figures also show the variations in the cyclic modulus for various contract pressures and plate diameters. Figure 4.10 shows that the cyclic modulus typically increases with increase in contact pressure for the 4 in. diameter plate for the specimens prepared with 10% to 20% fines contents.

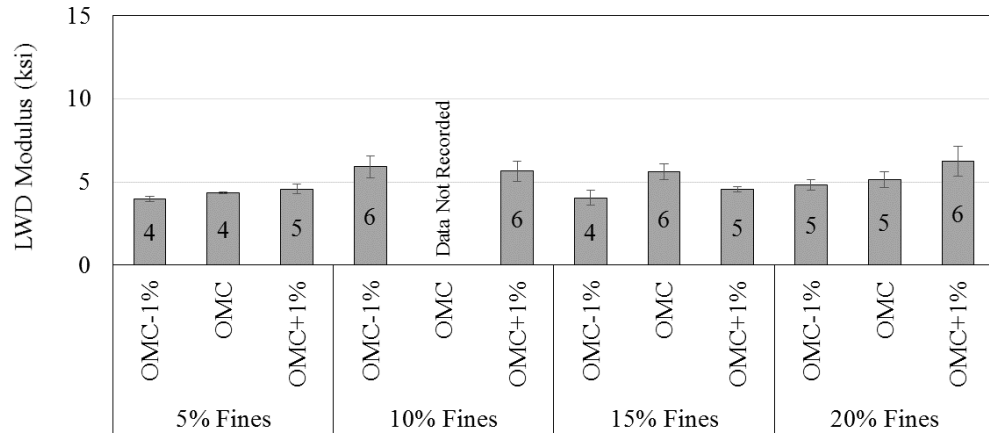


Figure 4.9 LWD modulus of subgrade

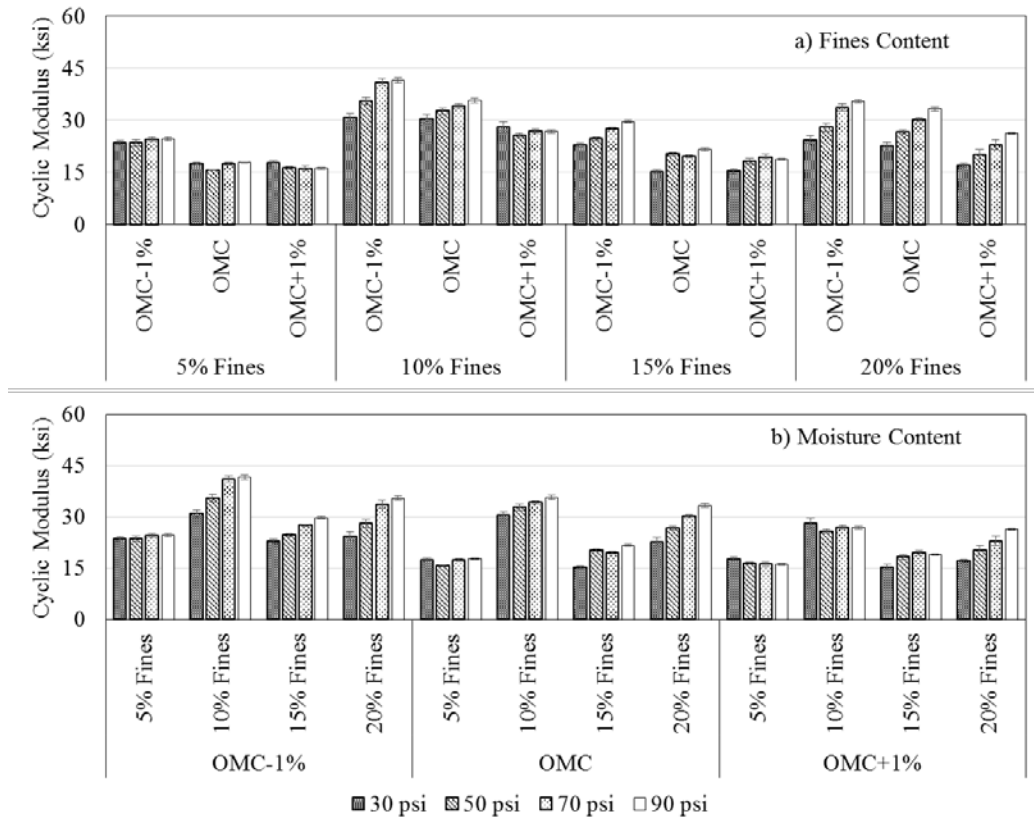


Figure 4.10 Cyclic modulus of large specimens from cyclic modulus test using 4” diameter plate: a) grouped by fines content and b) grouped by moisture content

The results also show that the cyclic modulus decreases with increase in moisture content in most instances. In the cases of test results with 8 in. and 12 in. diameter plates, the moduli increase with increase in contact pressure and slightly decrease or remain constant with increase in moisture (Figure 4.11 and Figure 4.12). Figure 4.10 through Figure 4.12 also show that the modulus of the specimen decreases with increase in the plate diameter. The decrease in the modulus is possibly

due to the influence of subgrade in the experiments. Furthermore, the maximum moduli were achieved with the specimens prepared at 10% fines content for all moisture contents.

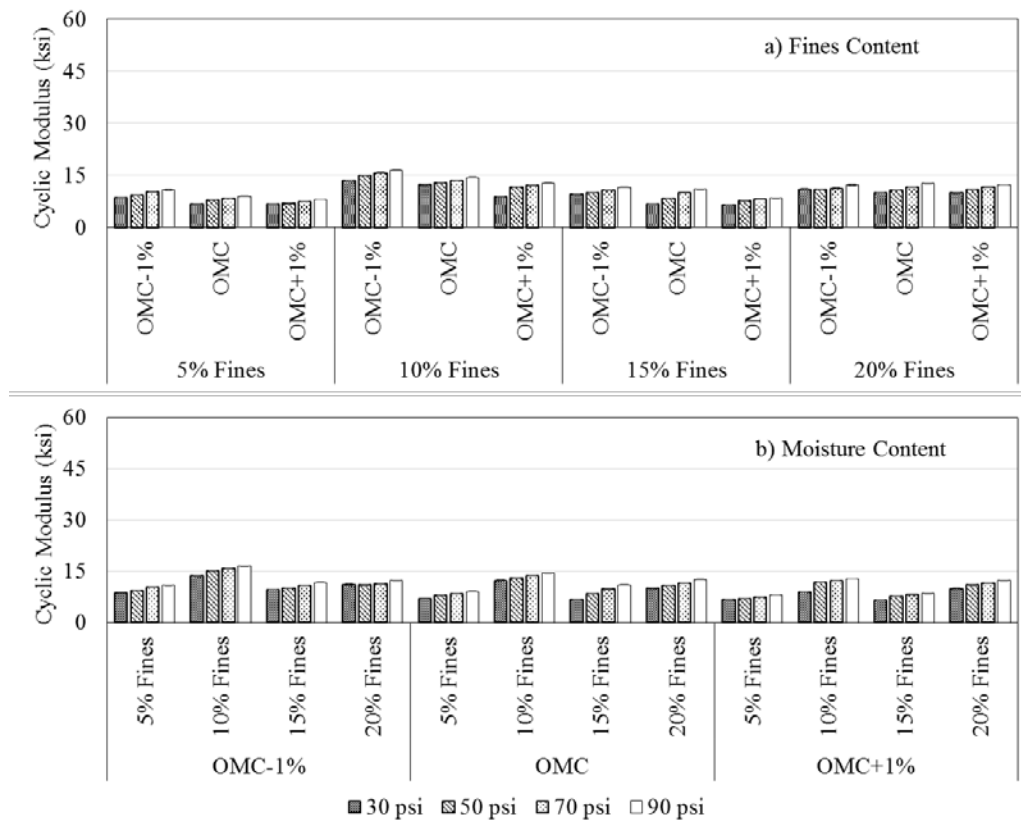


Figure 4.11 Cyclic modulus of large specimens from cyclic modulus test using 8” diameter plate: a) grouped by fines content and b) grouped by moisture content

Cyclic Stage Tests

Figure 4.13 shows the load-deformation responses of the base in the large specimens with the cyclic stage tests using various fines contents, moisture contents and loading conditions (cyclic-ramp load and continuous loads). The deformation of the specimens increases with increase in moisture content. The specimens prepared with 15% fines content deform highly at OMC+1% as compared to the other specimens prepared with different fines content and same moisture content. The specimen prepared with 15% fines content and moisture content of OMC+1% seemed highly wet as compared to all other specimens at OMC+1%. This is perhaps the reason for observing a high deformation. A clear trend of deformation with respect to changes in the fines content cannot be observed. The peak deformations of the specimens prepared with 10% and 20% fines contents are less than 80 mils and around 80 mils, respectively. However, the peak deformations for the specimens prepared with 5% and 15% fines contents are more than 80 mils. To understand these unusual deformational behaviors of bases with various moisture contents and fines contents, it is required to understand the soil-water-interaction of material at microscopic levels. In all tests, the continuous loads result in more deformations than the cyclic-ramp loads of the same magnitude.

Furthermore, the difference in the deformation responses due these two types of loads increases with increase in moisture content for the specimens prepared with 5% and 15% fines contents.

Figure 4.14 shows the variations of stiffness (measured from maximum load and corresponding deformation in the cyclic stage test) of the bases with fines content and moisture content. As the deformation due to the continuous load is greater than the cyclic-ramp load (Figure 4.13), the stiffness due to the continuous load is less than that of the cyclic-ramp load. The stiffness decreases with increase in moisture content for all fines content. The specimens prepared with 15% fines content are sensitive to change in moisture content, especially when the moisture content increases from OMC to OMC+1%. On the other hand, a reverse trend is evident for the specimens prepared with 20% fines content. From Figure 4.14b, the maximum stiffness is achieved for the specimens prepared with 10% fines contents at all moisture contents.

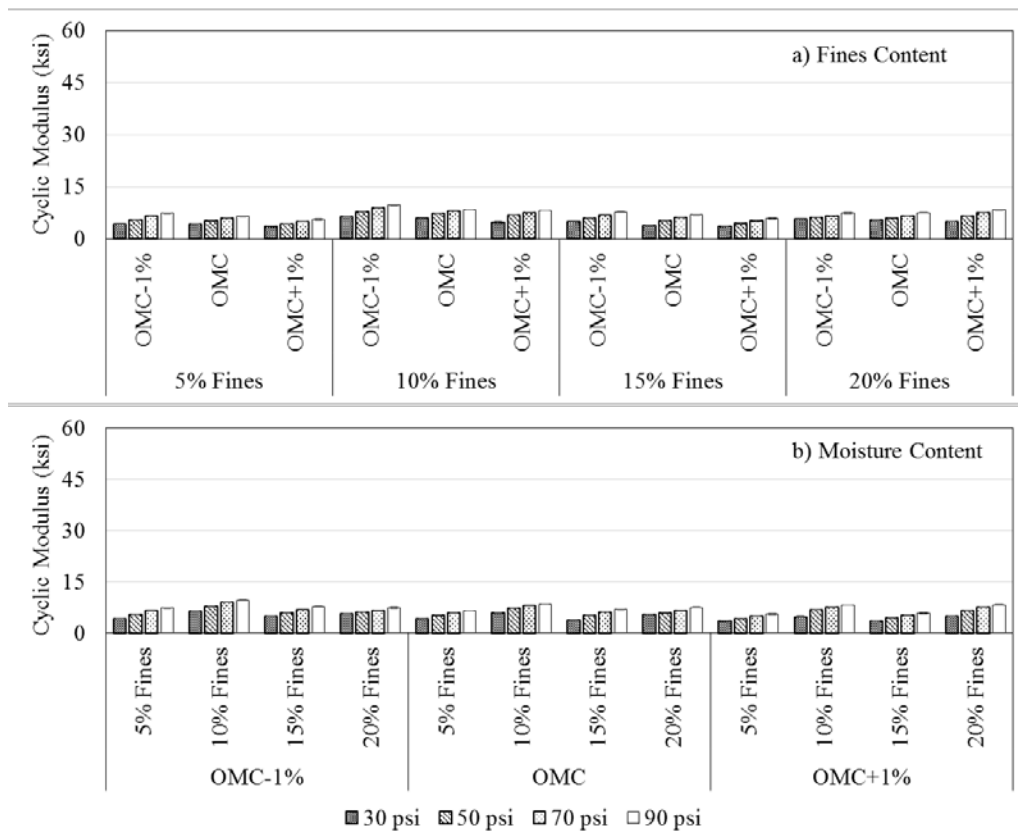


Figure 4.12. Cyclic modulus of large specimens from cyclic modulus test using 12'' diameter plate: a) grouped by fines content and b) grouped by moisture content

The variations in the permanent deformation (under the continuous load) of the large specimens with various fines content and moisture content are presented in Figure 4.15. The permanent deformation increases with increase in moisture content for all fines contents. The specimens prepared with 5% and 15% fines deform more significantly at OMC and OMC+1% as compared to the other specimens prepared at 10% and 20% fines contents. In general, the specimens prepared at 15% fines content are more sensitive to changes in the moisture content while a reverse behavior is observed for the specimens prepared at 20% fines content. Furthermore, the permanent

deformations of the specimens prepared at 15% fines content are only comparable with that of the standard specimens of the laboratory tests. The deformations in these specimens doubled when the moisture content increases from OMC-1% to OMC.

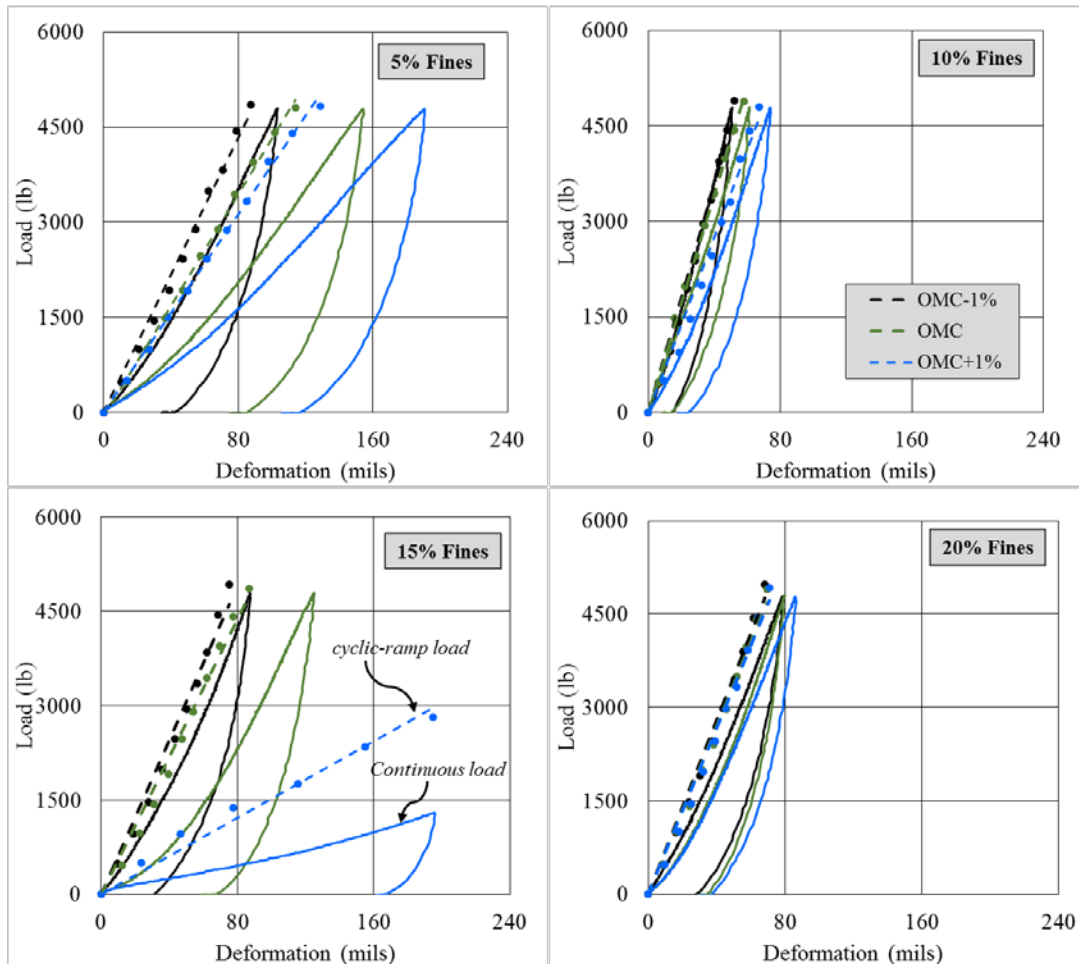


Figure 4.13 Load-deformation response of large specimens from cyclic stage test

Comparison of Laboratory and Small-Scale Tests

This section deals with the comparisons of the test results obtained from the laboratory and small-scale tests. These results are also correlated to understand the impact of the fines content and moisture content on the laboratory tests and small-scale tests.

Effect of Moisture Content on Laboratory Tests

The relationships between the normalized moduli, UCS and permanent deformation with the normalized moisture content of standard specimens are shown in Figure 4.16. The normalized modulus is defined as the ratio of the measured modulus at a given moisture content and the modulus at OMC. The UCS and permanent deformation are also normalized in a similar way. The normalized moisture content is the difference between the measured moisture content and OMC divided by OMC. As the resilient modulus and permanent deformation tests were conducted only at OMC-1% and OMC, few data are available for analyses (Figure 4.16c and Figure 4.16d). The normalized FFRC modulus, resilient modulus and UCS decrease with increase in moisture content.

The results also show that the FFRC modulus is more sensitive to the changes in the moisture content as compared to the resilient modulus and UCS. Figure 4.16d shows that the normalized permanent deformation increases with increase in moisture content. The correlation coefficients (R^2) for all cases are greater than 70% that indicate reasonably strong correlations between each test results and moisture content.

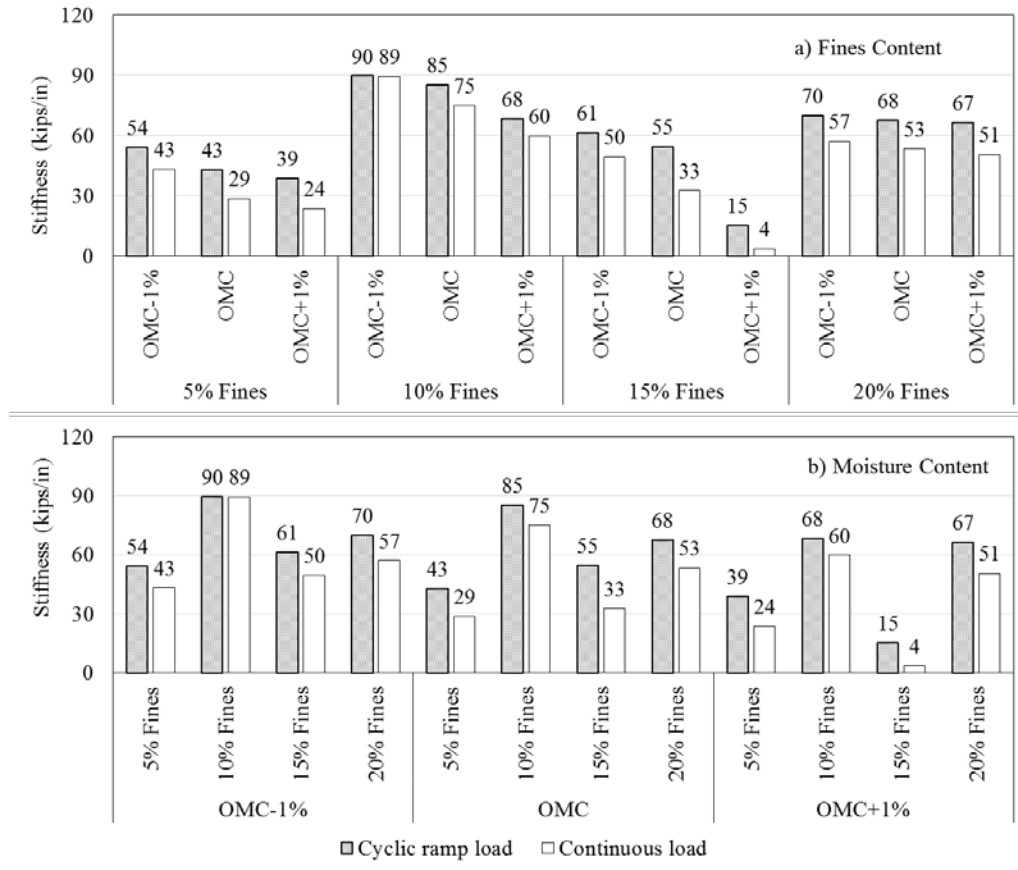


Figure 4.14 Stiffness of large specimens from cyclic stage test: a) grouped by fines content and b) grouped by moisture content

Effect of Moisture Content on Small-Scale Tests

Figure 4.17 shows the variations in normalized moduli, stiffness and permanent deformation with the normalized moisture content of large specimens. The stiffness is measured from the maximum load and corresponding deformation from the continuous load in cyclic stage test. As the PSPA tests were conducted only at OMC-1% and OMC, few data are available for analyses (Figure 4.17b). The increase in the moisture content results in decrease in the LWD and PSPA moduli (Figure 4.17a, Figure 4.17b). Both of these tests have reasonably good correlations. However, these relationships do not seem to be appropriate below a certain moisture content. Further, the stiffness values of the large specimens due to the continuous and cyclic ramp loads decrease with increase in the moisture content (Figure 4.17c). These stiffness values measured by the two loading methods at OMC are similar. However, the variations in the stiffness with moisture content are not as pronounced and well-defined as for the LWD and PSPA. Figure 4.17d shows that the permanent

deformation increases with increase in the moisture content. The result provides a reasonable correlation between the deformation and moisture content.

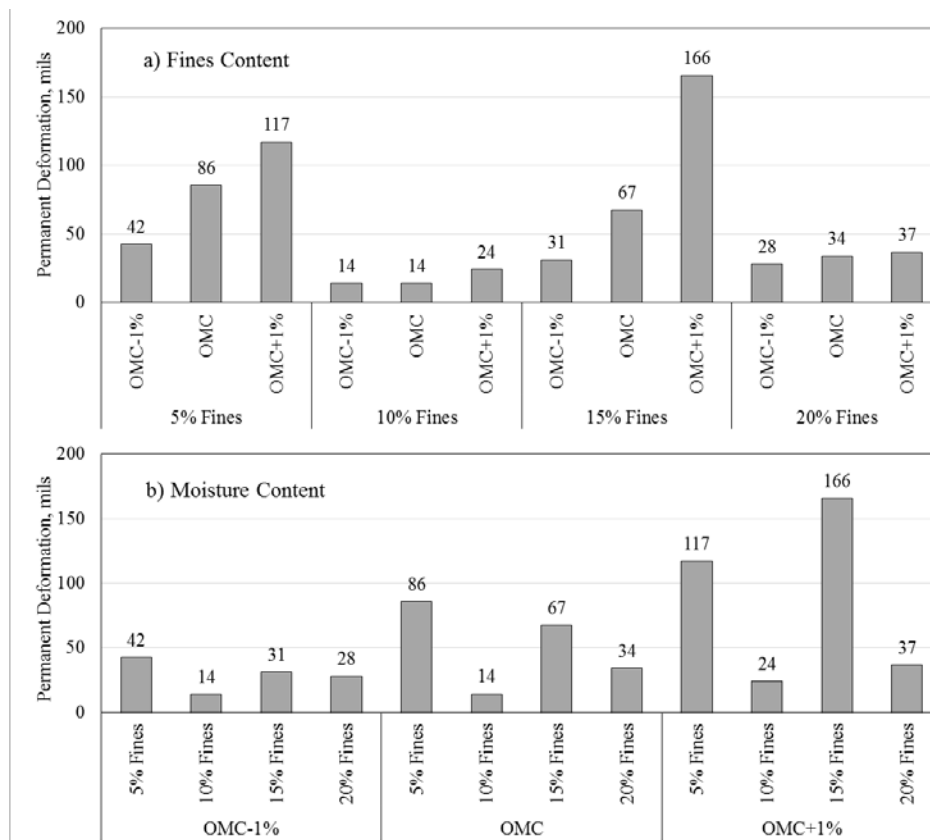


Figure 4.15 Permanent deformation of large specimens from cyclic stage tests: a) grouped by fines content and b) grouped by moisture content

Correlation of Laboratory Tests

The test results from the three types of laboratory tests (i.e., MR, FFRC and unconfined compression tests) are correlated in Figure 4.18. The resilient moduli are reasonably correlated with the FFRC moduli and UCS. However, a weaker correlation is observed between the FFRC modulus and UCS. The relationship between the resilient modulus and the FFRC modulus of geomaterials reported by (Nazarian et al. 2014) is also superimposed in Figure 4.18a. The two relationships differ from one another.

Correlation of Small-Scale Tests

The relations of the test results from the LWD and cyclic plate load tests are shown in Figure 4.19. As cyclic plate load tests were carried out with three different plate diameters (diameters of 4 in., 8 in. and 12 in.) using four different peak contact pressures (30 psi, 50 psi, 70 psi and 90 psi), a combination of twelve different relationships between the LWD modulus and the cyclic modulus are obtained. The R^2 typically increases with decrease in the plate diameter, except at the peak contact pressure of 30 psi. Further, the R^2 also typically increase with increase in the peak contact pressure from 50 psi to 90 psi. The results also indicate that the LWD moduli correlate reasonably

well with the cyclic moduli measured with the largest plate (12 in. diameter) and the highest peak contact pressure (90 psi).

The LWD used for the tests has 8 in. diameter plate and the peak contact pressure under the plate during the LWD test is approximately 34 psi. The cyclic modulus test with 8 in. diameter plate and 30 psi peak contact pressure is comparable with the LWD test. Interestingly, the LWD test results yielded the highest R^2 of 70% (see Figure 4.19a) with the cyclic modulus test conducted with 8 in. diameter plate at the peak contact pressure of 30 psi.

Figure 4.20 shows the variations in the LWD modulus with the stiffness measured on the large specimens in the cyclic stage tests. The results from the two plate load tests are reasonably correlated to the LWD modulus.

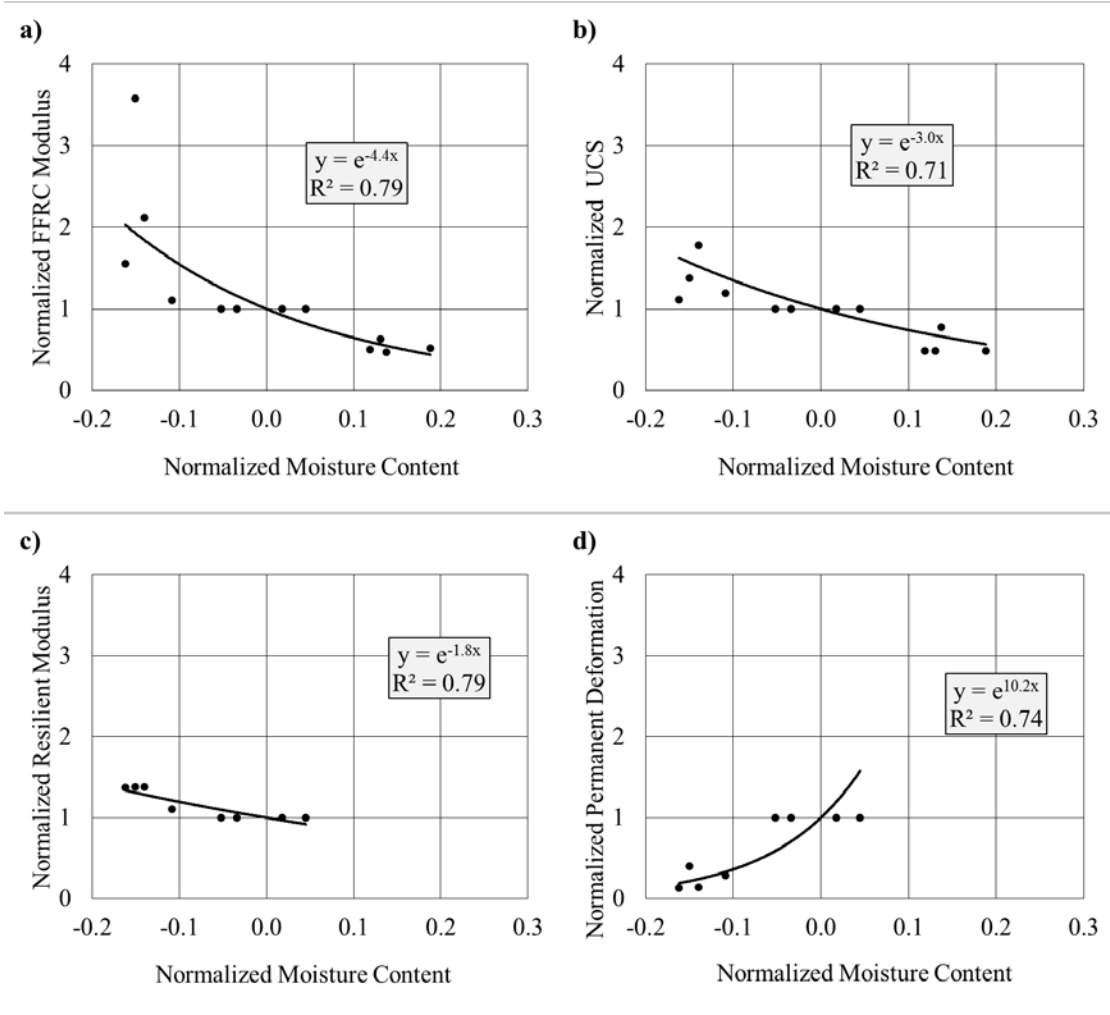


Figure 4.16. Variations in normalized moduli, UCS and permanent deformation with normalized moisture content in laboratory tests: a) FFRC Test, b) Unconfined Compression Test, c) Resilient Modulus Test and d) Permanent Deformation Test

Correlation of Laboratory Test and Small-Scale Tests

Figure 4.21 compares the permanent strains on the standard specimens from the laboratory tests with that of the large specimens from the small-scale tests. As permanent deformation tests on the

standard specimens were conducted only at OMC-1% and OMC, few data are available for analyses. The large specimens typically experience more permanent strains than the standard specimens. The permanent strains from the laboratory tests are poorly correlated with the small-scale tests.

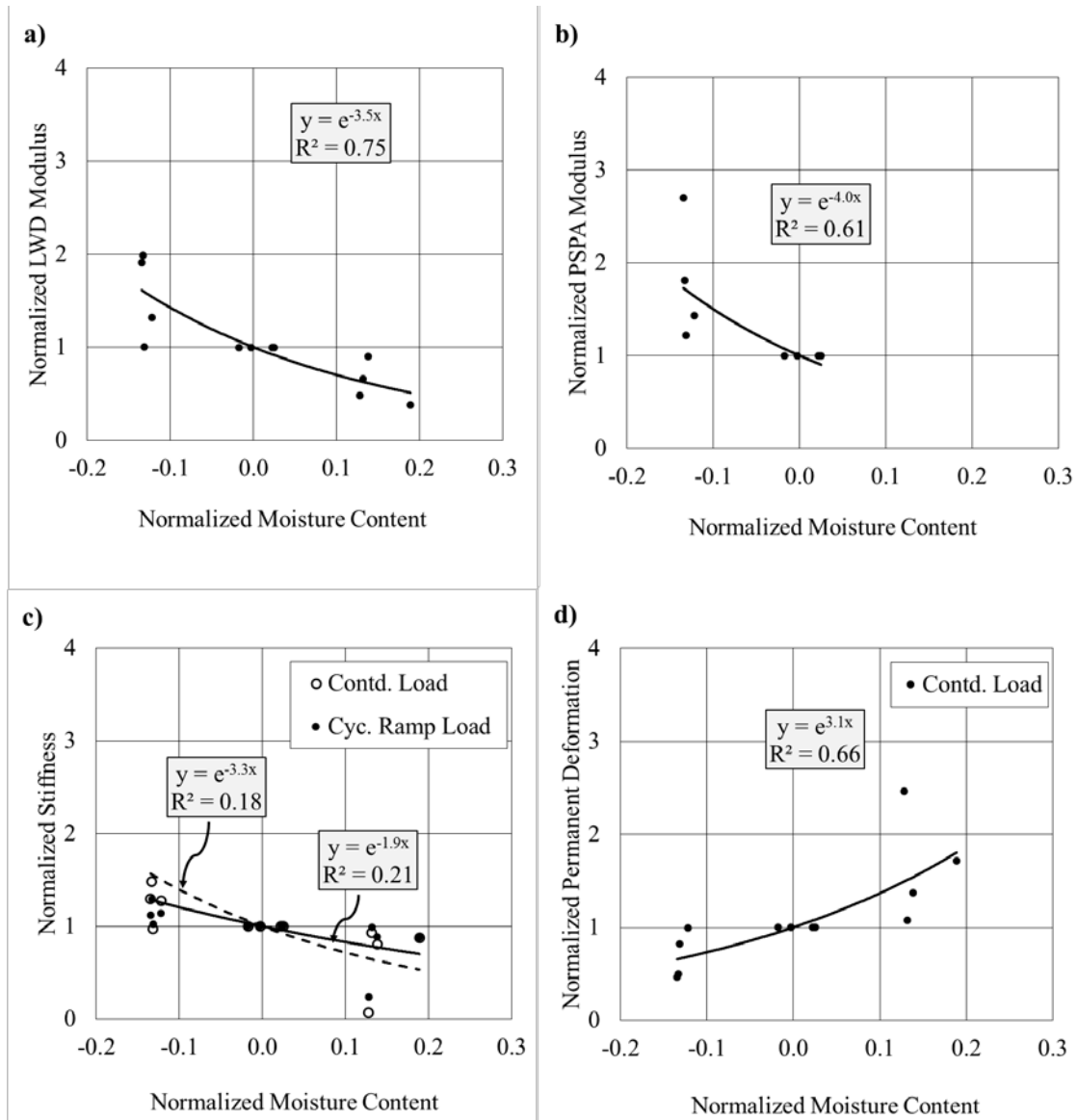


Figure 4.17 Variations in normalized modulus, permanent strain and stiffness with measured moisture content in small-scale tests: a) LWD Test, b) PSPA Test, c) Cyclic Modulus Test (CST) showing stiffness and d) CST showing permanent strain

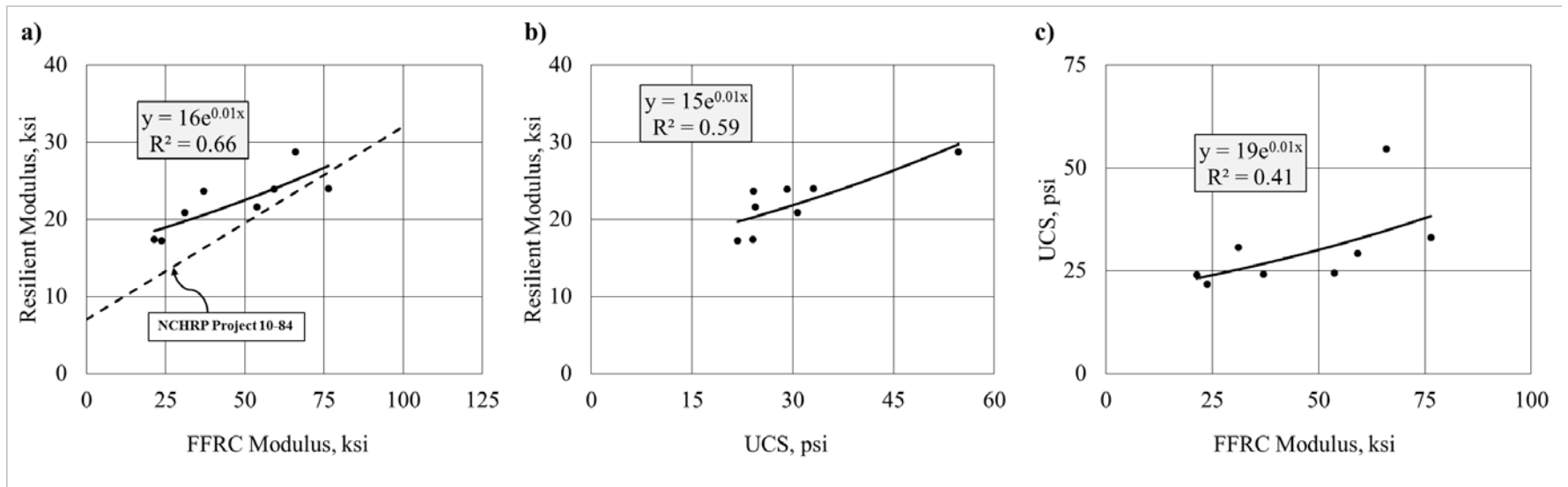


Figure 4.18 Variation in moduli and UCS of specimens in laboratory tests: a) Resilient Modulus (MR) Test and FFRC Test, b) MR Test and Unconfined Compression Test (UCT), and c) UCT and FFRC Test

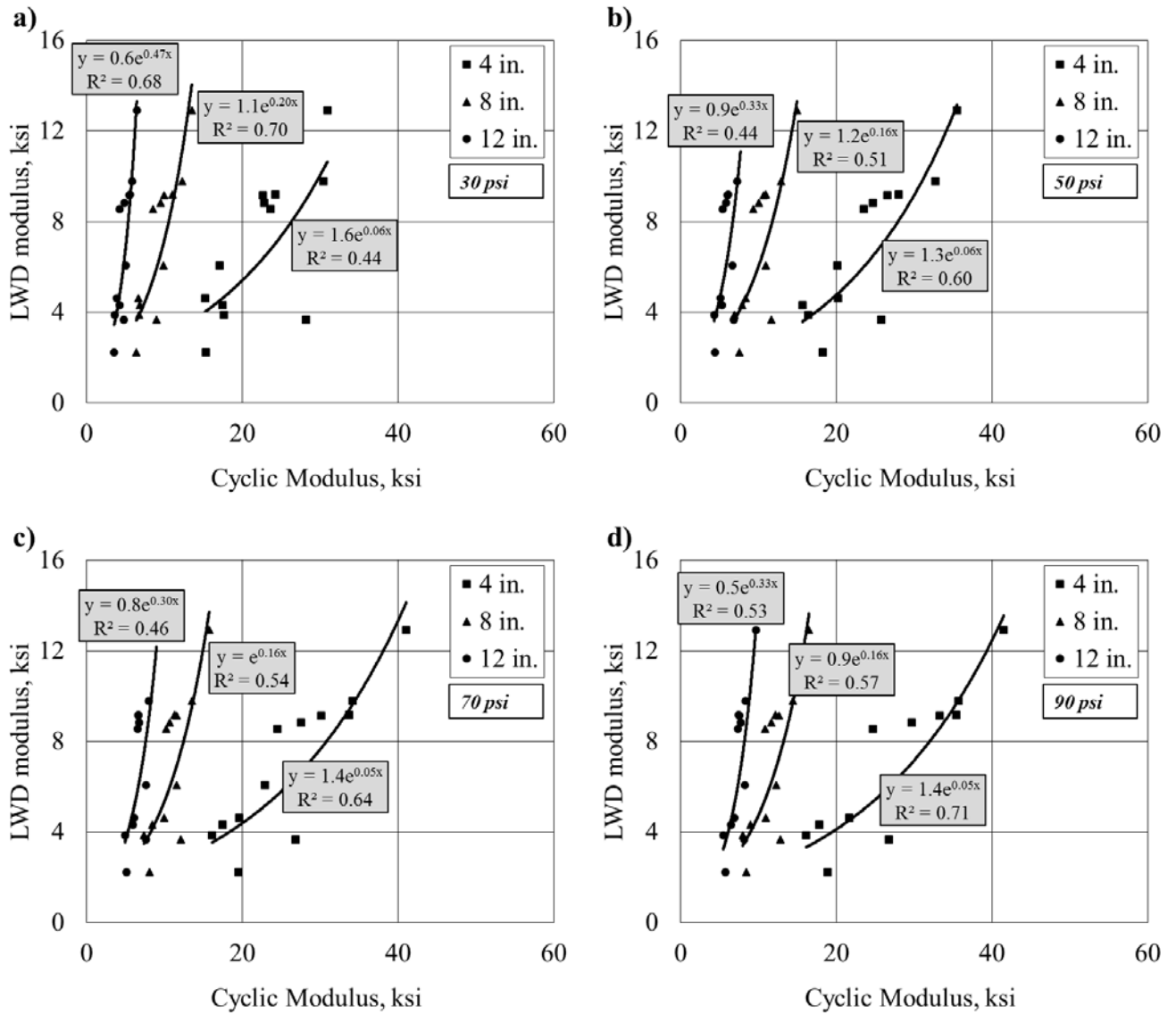


Figure 4.19 Variations in modulus of large specimens in small-scale tests with different loading plates at different peak contact pressures: a) 30 psi, b) 50 psi, c) 70 psi and d) 90 psi

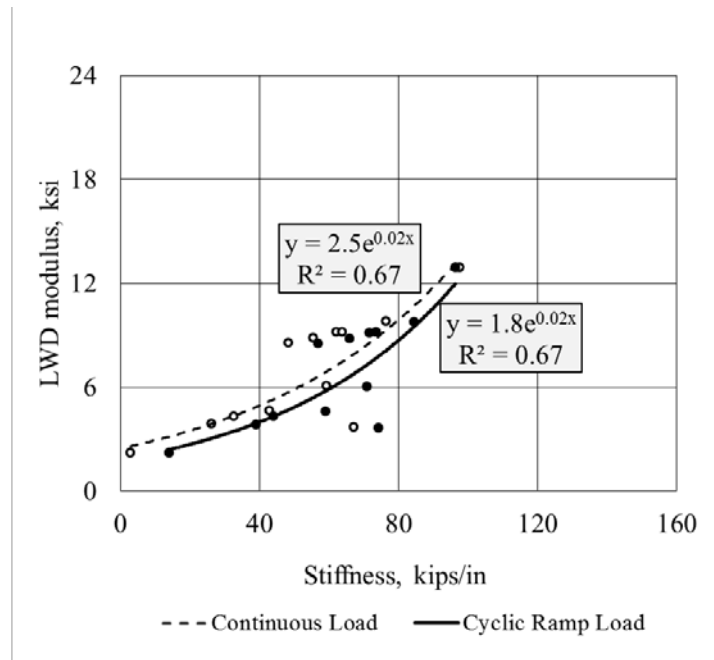


Figure 4.20 Variations in the LWD modulus and stiffness of large specimens measured through cyclic stage test in small-scale tests

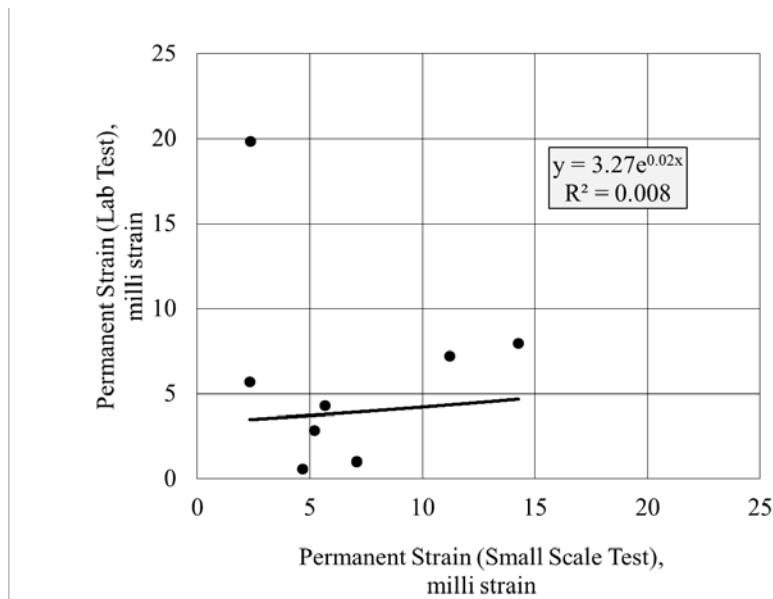


Figure 4.21 Variations in permanent strains of laboratory tests and small-scale tests:

Figure 4.22 shows the correlations between the k-parameters from the resilient modulus tests on the standard specimens and the permanent strains from the permanent deformation tests on the standard and large specimens. The k_2 and k_3 parameters have comparatively good correlation with the permanent strains from the standard laboratory specimens than those of the small-scale tests. On the other hand, the k_1 parameters are better correlated with the permanent strains of the large specimens. The permanent strains from the standard and large specimens gradually decrease with increase in the magnitude of k_1 parameter.

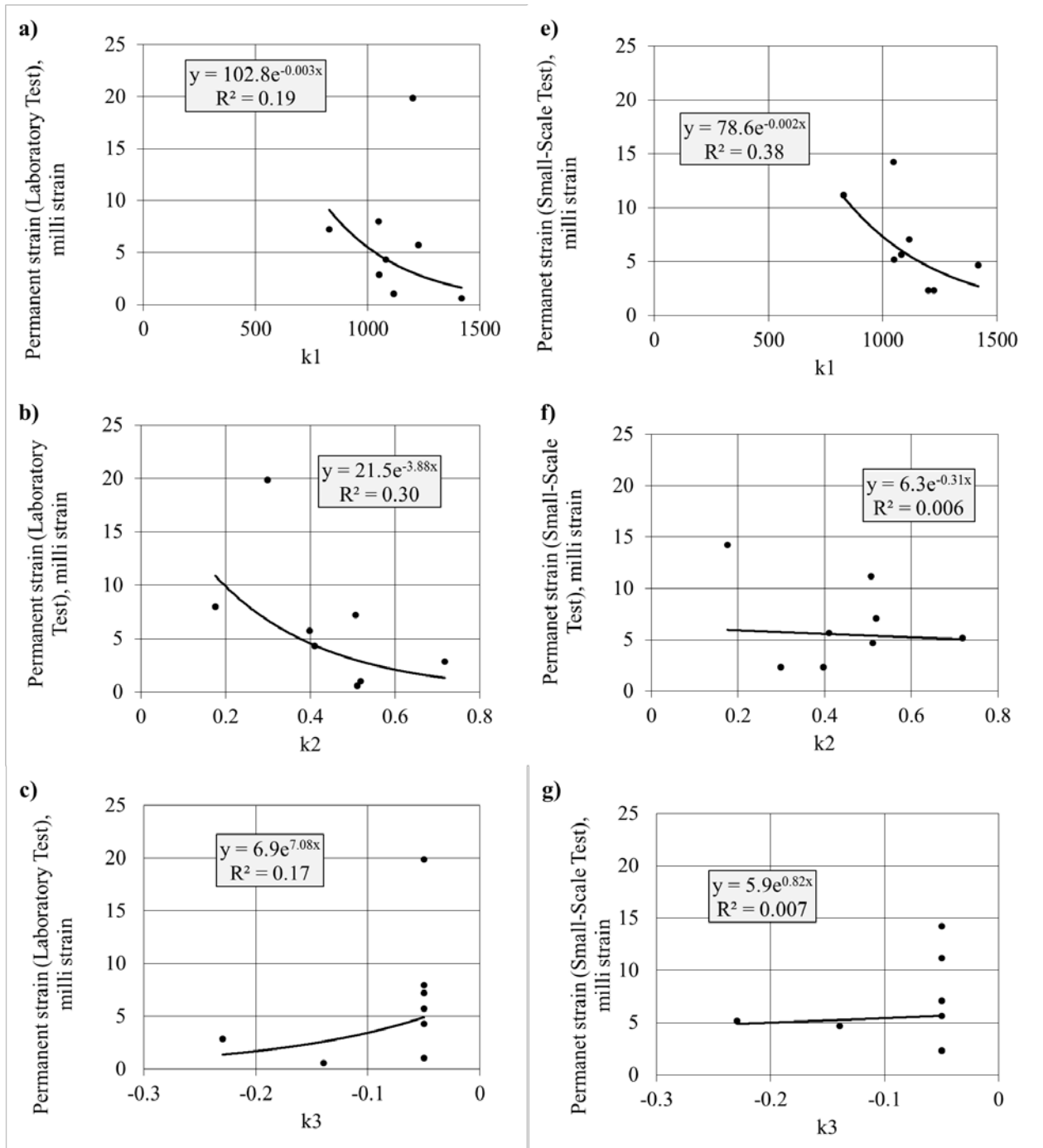


Figure 4.22 Variation of k-parameters with permanent strain measured from laboratory test (a, b and c). Variation of k-parameters with permanent strain measured in small-scale test (e, f and g)

Figure 4.23 compares the FFRC moduli of the standard specimens with the PSPA moduli of the large specimens. A good correlation between the two parameters are observed with the PSPA modulus being about 10% greater than the FFRC modulus.

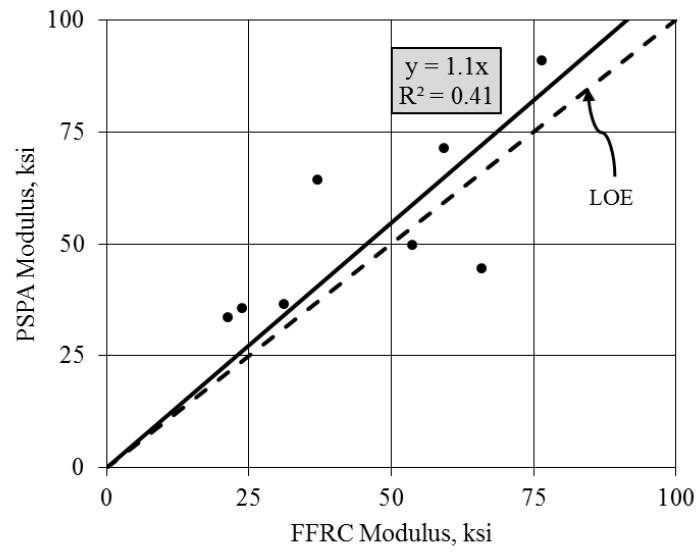


Figure 4.23 Variations in the PSPA modulus from small-scale test with the FFRC modulus from the laboratory test

Chapter 5 – Summary and Conclusions

The goal of this research was to understand the effects of fines content and moisture content on the strength and stability of geomaterial used in base layers of pavement. The specific research objectives were as follows:

- To evaluate the stiffness parameters of base materials with various fines contents and moisture contents;
- To understand the impact of the variations in fines content and moisture content of base materials on their performance;
- To develop a relationship among the stiffness parameters, fines contents and moisture content; and
- To correlate the stiffness parameters obtained from the laboratory and field methods

To achieve the stated goal and objectives, various experiments were carried out on the standard (6 in. in diameter and 12 in. in height) specimens in the laboratory tests and on the large (36 in. in diameter and 6 in. in height) specimens in the small-scale tests. The specimens for the tests were prepared with four different fines contents: 5%, 10%, 15% and 20%. The moisture contents for the tests were varied between OMC-1% and OMC+1%.

Based on the findings of the research, the following conclusions can be drawn:

- An increase in moisture content was typically detrimental to the mechanical properties of the base material. The strength and stiffness of material decreased due to increase in the moisture content. The increase in moisture content also resulted in the increase in the permanent deformation for all fines contents.
- The UCS, resilient modulus and FFRC modulus of standard specimens decreased with increase in moisture content.
- With the increase in fines content, the UCS increased for the standard specimens prepared at OMC-1% and OMC, and the FFRC modulus increased only at OMC-1%. However, the resilient moduli were not as highly affected by the change in fines content.
- The permanent deformation of the standard specimens increased with increase in moisture content for all fines contents. The permanent deformation typically decreased with increase in fines content.
- The PSPA, LWD and cyclic moduli measured on large specimens typically decreased with increase in moisture content. The maximum PSPA moduli were achieved for the specimens prepared with the fines contents between 10% to 15% whereas the maximum LWD and cyclic moduli were achieved at 10% fines content.
- The cyclic moduli were also impacted by the loading area (the plate diameter) and imposed load (the peak contact pressure).
- As in the laboratory tests, the permanent deformation of the large specimens (in the small-scale tests) during cyclic stage tests increased with increase in moisture content. However, no definite pattern of deformation on the large specimens was observed with increase in fines content.
- The stiffness measured with the cyclic ramp load was greater than that from the continuous load.
- In the laboratory tests, the resilient moduli showed reasonably good correlation with the FFRC moduli and UCS.

- In the small-scale tests, the LWD moduli correlated reasonably well with the cyclic moduli measured with the largest plate (12 in. diameter) and highest peak contact pressure (90 psi) in the cyclic modulus tests.
- The FFRC moduli measured in the laboratory tests showed a good correlation with the PSPA moduli measured in the small-scale tests.
- The permanent deformations measured in the laboratory tests showed poor correlations with that of the small-scale tests.

References

- Alshibli, K. A., Abu-Farsakh, M., and Seyman, E. (2005). "Laboratory Evaluation of the Geogauge and Light Falling Weight Deflectometer as Construction Control Tools." *Journal of Materials in Civil Engineering*, American Society of Civil Engineers, 17(5), 560–569.
- Amiri, H., Nazarian, S., and Fernando, E. (2009). "Investigation of Impact of Moisture Variation on Response of Pavements through Small-Scale Models." *Journal of Materials in Civil Engineering*, American Society of Civil Engineers, 21(10), 553–560.
- Barskale, R. D., and Itani, S. Y. (1989). "Influence of aggregate shape on base behavior." *Transportation Research Record*, (1227), 173–182.
- Bilodeau, J., Dore, G., and Pierre, P. (2009). "Pavement base unbound granular materials gradation optimization." *Bearing Capacity of Roads, Railways and Airfields. 8th International Conference*, 145–154.
- Brown, S. F., and Chan, F. W. K. (1996). "Reduced Rutting in Unbound Granular Pavement Layers Through Improved Grading Design." *Proceedings of the ICE - Transport*, Thomas Telford, 117(1), 40–49.
- Buchanan, S. (2007). "Resilient Modulus: What, Why, and How." *Vulcan Materials Company*, 1–13.
- Cary, C. E., and Zapata, C. E. (2010). "Enhanced model for resilient response of soils resulting from seasonal changes as implemented in mechanistic-empirical pavement design guide." *Transportation Research Record: Journal of the Transportation Research Board*, 2170(1), 36–44.
- Celaya, M., Nazarian, S., and Yuan, D. (2006). "Nondestructive Quality Control of Geo-Materials Using Seismic Methods." *Geotechnical Special Publication*, Reston, VA; American Society of Civil Engineers; 1998, 149, 182.
- Cooper, K. E., Brown, S. F., and Pooley, G. R. (1985). "The Design of Aggregate Gradings for Asphalt Base courses." *Association of Asphalt Paving Technologists Proc.*, 324–346.

- Dawson, A., Mundy, M., and Huhtala, M. (2000). "European research into granular material for pavement bases and subbases." *Transportation Research Record: Journal of the Transportation Research Board*, (1721), 91–99.
- Dawson, A. R., Thom, N. H., and Paute, J. L. (1996). "Mechanical characteristics of unbound granular materials as a function of condition." *Gomes Correia, Balkema, Rotterdam*, 35–44.
- DeMerchant, M. R., Valsangkar, A. J., and Schriver, A. B. (2002). "Plate load tests on geogrid-reinforced expanded shale lightweight aggregate." *Geotextiles and Geomembranes*, 20(3), 173–190.
- Ekblad, J., and Isacsson, U. (2006). "Influence of water on resilient properties of coarse granular materials." *Road materials and pavement design*, 7(3), 369–404.
- Fleming, P. R., Frost, M. W., Rogers, C. D. F., Thom, N. H., and Armitage, R. J. (2000). "Performance based specification for road foundation materials." *Institute of Quarrying Millennium Conference*, Bristol.
- Gandara, J. A. (2004). "Characterization of Texas bases through permanent deformation testing." *University of Texas at El Paso*, El Paso, TX.
- Gandara, J., and Nazarian, S. (2006). "Characterization of Rutting Potential of Texas Bases Through Laboratory and Small-Scale Tests." *Transportation Research Board 85th Annual Meeting*, 1–15.
- Gautam, B., Yuan, D., Abdallah, I., and Nazarian, S. (2009). *Guidelines for using local material for roadway base and subbase*. Research Report 0-5562-1, Center for Transportation Infrastructure Systems, The University of Texas at El Paso, El Paso, TX.
- Ghabchi, R., Zaman, M., Khoury, N., Kazmee, H., and Solanki, P. (2013). "Effect of gradation and source properties on stability and drainability of aggregate bases: a laboratory and field study." *International Journal of Pavement Engineering*, Taylor & Francis Group, 14(3), 274–290.
- Gidel, G., Horny, P., Chauvin, J.-J., Breysse, D., and Denis, A. (2001). "A new approach for investigating the permanent deformation behavior of unbound granular material using the Repeated Load Triaxial Apparatus." *Bulletin de Liaison des Laboratoires des Ponts et Chaussées*, 233, 5–21.
- Gray, J. E. (1962). "Characteristics of graded base course aggregates determined by triaxial tests." *Engineering Research Bulletin No. 12*, National Crushed Stone Association, Alexandria, VA.
- Habiballah, T., and Chazallon, C. (2005). "An elastoplastic model based on the shakedown concept for flexible pavements unbound granular materials." *International Journal for Numerical and Analytical Methods in Geomechanics*, 29(6), 577–596.

- Hicks, R. G., and Monismith, C. L. (1971). "Factors influencing the resilient response of granular materials." *Highway research record*, (345), 15–31.
- Huang, C.-W., Al-Rub, R. K. A., Masad, E. A., and Little, D. N. (2010). "Three-dimensional simulations of asphalt pavement permanent deformation using a nonlinear viscoelastic and viscoplastic model." *Journal of Materials in Civil Engineering*, 23(1), 56–68.
- Ishihara, K. (1996). *Soil behaviour in earthquake geotechnics*. Oxford University Press, Oxford, UK.
- Jorenby, B. N., and Hicks, R. G. (1986). "Base Course Contamination Limits." *Transportation Research Record*, (1095), 86–101.
- Kamal, M. A., Dawson, A. R., Farouki, O. T., Hughes, D., and Sha'at, A. A. (1993). "Field and laboratory evaluation of the mechanical behavior of unbound granular materials in pavements." *Transportation Research Record*, (1406), 88–97.
- Karasahin, M., Dawson, A. R., and Holden, J. T. (1993). "Applicability of resilient constitutive models of granular material for unbound base layers." *Transportation Research Record*, (1406), 98–107.
- Kaya, Z., Cetin, A., Cetin, B., Aydilek, A. H., and others. (2012). "Effect of Compaction Method on Mechanical Behavior of Graded Aggregate Base Materials." *GeoCongress 2012@ State of the Art and Practice in Geotechnical Engineering*, 1486–1494.
- Kolisoja, P. (1997). "Resilient deformation characteristics of granular materials." University of Technology, Tampere, Finland.
- Konrad, J.-M., and Lemieux, N. (2005). "Influence of fines on frost heave characteristics of a well-graded base-course material." *Canadian geotechnical journal*, NRC Research Press, 42(2), 515–527.
- Lekarp, F. (1999). "Resilient and permanent deformation behavior of unbound aggregates under repeated loading." Royal Institute of Technology, Stockholm, Sweden.
- Lekarp, F., Isacsson, U., and Dawson, A. (2000). "State of the art. I: Resilient response of unbound aggregates." *Journal of Transportation Engineering*, 126(1), 66–75.
- Li, T., and Baus, R. L. (2005). "Nonlinear Parameters for Granular Base Materials from Plate Tests." *Journal of Geotechnical and Geoenvironmental Engineering*, American Society of Civil Engineers, 131(7), 907–913.
- Malla, R. B., and Joshi, S. (2008). "Subgrade resilient modulus prediction models for coarse and fine-grained soils based on long-term pavement performance data." *International Journal of Pavement Engineering*, 9(6), 431–444.

- Mazari, M., Navarro, E., Abdallah, I., and Nazarian, S. (2014). "Comparison of numerical and experimental responses of pavement systems using various resilient modulus models." *Soils and Foundations*, 54(1), 36–44.
- Nazarian, S., Mazari, M., Abdallah, I. N., Puppala, A. J., and Mohammad, L. N. (2014). *Modulus-based construction specification for compaction of earthwork and unbound aggregate*. Transportation Research Board, Draft Interim Report for NCHRP Project 10-84.
- Nazarian, S., Yuan, D., and Williams, R. R. (2003). "A simple method for determining modulus of base and subgrade materials." *ASTM Special Technical Publication*, 1437, 152–164.
- Pan, T., Tutumluer, E., and Anochie-Boateng, J. (2006). "Aggregate morphology affecting resilient behavior of unbound granular materials." *Transportation Research Record: Journal of the Transportation Research Board*, (1952), 12–20.
- Piratheepan, J., Gnanendran, C. T., and Lo, S.-C. R. (2010). "Characterization of Cementitious Stabilized Granular Materials for Pavement Design Using Unconfined Compression and IDT Testings with Internal Displacement Measurements." *Journal of Materials in Civil Engineering*, American Society of Civil Engineers, 22(5), 495–505.
- Von Quintus, H. L., Rao, C., Minchin, R. E., Nazarian, S., Maser, K. R., and Prowell, B. (2009). *NDT technology for quality assurance of HMA pavement construction*. Transportation Research Board.
- Von Quintus, H., and Killingsworth, B. (1998). *Analyses relating to pavement material characterizations and their effects on pavement performance*. Federal Highway Administration, McLean, VA.
- Raad, L., Minassian, G. H., and Gartin, S. (1992). *Characterization of saturated granular bases under repeated loads*. Transportation Research Record 1369, Washington, D.C.
- Richter, C. A. (2006). "Seasonal variations in the moduli of unbound pavement layers." Report No. FHWA-HRT-04-079, Federal Highway Administration, U.S. Department of Transportation.
- Saeed, A., Hall, J. W., and Barker, W. (2001). "NCHRP Report 453: Performance-Related Tests of Aggregates for Use in Unbound Pavement Layers." *Transportation Research Board, National Research Council, Washington, DC*, 1–56.
- Salehi, R., Little, D., and Masad, E. (2008). "Material Factors That Influence Anisotropic Behavior of Aggregate Bases." *Transportation Research Record: Journal of the Transportation Research Board*, Transportation Research Board of the National Academies, 2059, 20–30.
- Santha, B. (1994). "Resilient modulus of subgrade soils: comparison of two constitutive equations." *Transportation Research Record*, (1462), 79–90.

- Sawangsuriya, A., Bosscher, P. J., and Edil, T. B. (2006). "Alternative Testing Techniques for Modulus of Pavement Bases and Subgrades." *13th Great Lakes Geotechnical and Geoenvironmental Conference*, 108–121.
- Schnaid, F., Prietto, P. D. M., and Consoli, N. C. (2001). "Characterization of Cemented Sand in Triaxial Compression." *Journal of Geotechnical and Geoenvironmental Engineering*, American Society of Civil Engineers, 127(10), 857–868.
- Simpson, A. (1999). "Characterization of transverse profile." *Transportation Research Record: Journal of the Transportation Research Board*, Transportation Research Board of the National Academies, (1655), 185–191.
- Stokoe, K. H., Wright, S. G., Bay, J. A., and Roesset, J. M. (1994). "Characterization of geotechnical sites by SASW method." *Geophysical characterization of sites*, 15–25.
- Sweere, G. T. H. (1990). "Unbound granular bases for roads." TU Delft, Delft University of Technology.
- Thom, N. H., and Brown, S. F. (1988). "The effect of grading and density on the mechanical properties of a crushed dolomitic limestone." *Australian Road Research Board (ARRB) Conference, 14th, 1988, Canberra*, 94–100.
- Thompson, M. R., and Smith, K. L. (1990). "Repeated triaxial characterization of granular bases." National Research Council, Washington, D.C., 7–17.
- Tian, P., Zaman, M., and Laguros, J. (1998). "Gradation and moisture effects on resilient moduli of aggregate bases." *Transportation Research Record: Journal of the Transportation Research Board*, (1619), 75–84.
- Tutumluer, E. (2013). *Practices for unbound aggregate pavement layers*. NCHRP Synthesis 445, National Cooperative Highway Research Program, Transportation Research Board., Washington, D.C.
- Tutumluer, E., and Seyhan, U. (2000). "Effects of fines content on the anisotropic response and characterization of unbound aggregate bases." *Proceedings of the Unbound Aggregates in Roads (UNBAR5) Symposium, University of Nottingham, England*.
- Wen, H., Warner, J., Edil, T., and Wang, G. (2010). "Laboratory Comparison of Crushed Aggregate and Recycled Pavement Material With and Without High Carbon Fly Ash." *Geotechnical and Geological Engineering*, 28(4), 405–411.
- White, D. J., Morris, M., and Thompson, M. (2006). "Power-Based Compaction Monitoring Using Vibratory Padfoot Roller." *GeoCongress 2006*, 1–6.

- Williams, R. R., and Nazarian, S. (2007). "Correlation of Resilient and Seismic Modulus Test Results." *Journal of Materials in Civil Engineering*, American Society of Civil Engineers, 19(12), 1026–1032.
- Yau, A., and Quintus, H. L. Von. (2002). "Study of LTPP laboratory resilient modulus test data and response characteristics." Report No. FHWA-RD-02-051, Federal Highway Administration, Austin, TX.
- Yideti, T. F., Birgisson, B., Jelagin, D., and Guarin, A. (2014). "Packing theory-based framework for evaluating resilient modulus of unbound granular materials." *International Journal of Pavement Engineering*, Taylor & Francis, 15(8), 689–697.
- Yuan, D., and Nazarian, S. (2003). "Variation in moduli of base and subgrade with moisture." *Transportation Research Board 82nd Annual Meeting, Washington, DC*, 12–16.